

**Lower to Middle Ordovician carbonate  
sedimentology and stratigraphy of the  
Pakri peninsula, north-western  
Estonia**

***Niklas Brådenmark***

**Dissertations in Geology at Lund University,  
Master's thesis, no 489  
(45 hp/ECTS credits)**



**Department of Geology  
Lund University  
2016**



**Lower to Middle Ordovician  
carbonate sedimentology and  
stratigraphy of the Pakri peninsula,  
north-western Estonia**

Master's thesis  
Niklas Brådenmark

Department of Geology  
Lund University  
2016

# Contents

<b>1 Introduction</b> .....	<b>7</b>
<b>2 Geological setting</b> .....	<b>7</b>
<b>3 Stratigraphy of northern Estonia</b> .....	<b>7</b>
<b>4 Depositional cycles</b> .....	<b>10</b>
<b>5 Materials and methods</b> .....	<b>10</b>
<b>6 Sedimentary petrography of the Uuga cliff section and the Testepere quarry</b> .....	<b>11</b>
6.1 Toila Formation	11
6.2 Pakri Formation	11
6.3 Aseri Formation	15
6.4 Vão Formation	16
6.5 Kõrgekallas Formation	17
<b>7 Sedimentary Petrography of the Tabasalu road cut section</b> .....	<b>17</b>
7.1 Toila Formation	17
7.2 Pakri Formation	20
7.3 Aseri Formation	21
7.4 Vão Formation	21
<b>8 Stable carbon isotope data</b> .....	<b>22</b>
<b>9 Discussion</b> .....	<b>24</b>
9.1.1 Leetse Formation	24
9.1.2 Toila Formation	26
9.1.3 Pakri Formation	26
9.1.4 Aseri Formation	27
9.1.5 The Vão and Kõrgekallas formations	27
9.2 Cool water carbonates and carbonate sedimentation in Baltoscandia	27
<b>10 Conclusions</b> .....	<b>28</b>
<b>11 Acknowledgements</b> .....	<b>28</b>
<b>12 References</b> .....	<b>28</b>
<b>13 Appendix</b> .....	<b>31</b>

**Cover Picture:** Overview of the Uuga cliff section in June 2014 (photograph: O. Lehnert).

# Lower to Middle Ordovician carbonate sedimentology and stratigraphy of the Pakri peninsula, north-western Estonia

Niklas Brådenmark

Brådenmark, N., 2016: Lower to Middle Ordovician carbonate sedimentology and stratigraphy of the Pakri peninsula, north-western Estonia. *Dissertations in Geology at Lund University*, No. 489, 33 pp. 45 hp (45 ECTS credits).

**Abstract:** The sedimentology and stratigraphy of the latest Early Ordovician through Middle Ordovician of north-western Estonia has been investigated. The study encompasses coastal cliff sections and the Testepere quarry on the Pakri peninsula, as well as a road-cut outside the town of Tabasalu just west of Tallinn. The exposed successions represent a low relief epeiric carbonate ramp developed in the Baltoscandian basin. Study of carbonate microfacies, hardgrounds and glauconite content indicates a sea level highstand during the Volkhov (Dapingian) or Kunda stages (early Darriwilian) and a sea level drop coinciding with the Volkhov-Kunda boundary. Slow or non-deposition is marked by the high content of glauconite and/or hardgrounds. The glauconite content is highest in the Leetse Formation but exists in high amounts also all the way through the Pakri Formation. Hardgrounds are mostly of corroded character but abraded hardgrounds are present, such as the widespread “Püstakkiht” hardground complex, which marks the Floian-Dapingian boundary in the Toila Formation.

**Keywords:** bedrock geology, Ordovician, Baltoscandian basin, sea level, limestone, hardgrounds, glauconite.

**Supervisors:** Mikael Calner, Oliver Lehnert

**Subject:** Bedrock Geology

*Niklas Brådenmark, Department of Geology, Lund University, Sölvegatan 12, SE-223 62 Lund, Sweden. E-mail: nbradenmark@gmail.com*

# Lower to Middle Ordovician carbonate sedimentology and stratigraphy of the Pakri peninsula, north-western Estonia

Niklas Brådenmark

Brådenmark, N., 2016: Lower to Middle Ordovician carbonate sedimentology and stratigraphy of the Pakri peninsula, north-western Estonia. *Examensarbeten i geologi vid Lunds universitet*, Nr. 489, 33 sid. 45 hp.

**Sammanfattning:** Sedimentologi och stratigrafi från senaste tidiga ordovicium till och med mellanordovicium i nordvästra Estland har undersökts. Studien omfattar klippsektioner och Testepere stenbrott på Pakrihalvön, samt en vägskärning utanför staden Tabasalu strax väster om Tallinn. De exponerade lagerföljderna representerar en epeirisk karbonatramp med låg relief som utvecklats i det baltoskandiska grundhavet. Studier av karbonatmikrofacies, hårdbottnar och dess glaukonitnehåll indikerar högst havsnivåer under etagera Volkhov (Dapingian) och Kunda (tidig Darriwilian). Lägre havsnivå sammanfaller med gränsen mellan etagera Volkhov och Kunda. Långsam eller ingen avsättning kännetecknas av den höga halten av glaukonit och/eller hårdbottnar. Glaukonitnehållet är högst i Leetseformationen men förekommer i stora mängder hela vägen till och med Pakriformationen. Hårdbottnar är mestadels av korroderad typ men abraderade förekommer också. Ett exempel på en serie abraderade hårdbottnar är den utbredda "Püstakkiht", i Toilaformationen som markerar gränsen mellan Floian-Dapingian.

**Nyckelord:** berggrundsgeologi, ordovicium, baltoskandiska grundhavet, havsnivå, kalksten, glaukonit hårdbottnar.

**Handledare:** Mikael Calner, Oliver Lehnert

**Ämnesinriktning:** Berggrundsgeologi

*Niklas Brådenmark, Department of Geology, Lund University, Sölvegatan 12, SE-223 62 Lund, Sweden. E-mail: nbradenmark@gmail.com*

# 1 Introduction

The Lower-Middle Ordovician was a time period of high global sea level, at least 100-170 metres higher than present (Miller et al. 2005). This can be considered exceptionally high since global sea level changes of the early Phanerozoic rarely exceed an amplitude of 150 m and many are about 75 m or less (Haq & Schutter 2008). Due to the high sea-level, extensive parts of the continents, including the Baltoscandian region, were submerged. Certain authors (Artyushkov et al. 2000) report that sea level in the Baltoscandian basin may have fluctuated by as much as 150 metres between highstand and lowstand periods. This basin was an exceptionally sediment-starved and slowly subsiding, shallow epicontinental basin surrounded by a low relief hinterland (Calner et al. 2014). For this reason, eustatic sea level fluctuations played an important role in the formation and facies architecture of the sedimentary successions (Dronov & Holmer 1999). On a global scale, sea level rose during the Tremadocian and peaked in Floian whereafter it became successively lower throughout the Dapingian and Darriwilian stages. It reached a lowstand sometime during the Darriwilian or Sandbian stages (Munnecke et al. 2010). The sedimentary record of the Baltoscandian basin reflects such sea-level evolution. While many authors (Nielsen 2003; Dronov 2005) agree on a general sea level rise during the Early Ordovician up to the latest Floian, there is some disagreement regarding the magnitude of regressions within the Lower and Middle Ordovician and for the latter period interpretations of the Baltoscandian sea level history differ drastically. Nielsen (2003) argues for a large-scale regression throughout the whole Middle Ordovician whereas Dronov suggests a highstand throughout this time interval. According to Nielsen (2003), the sea level drop at the base of the Dapingian is one of the more prominent ones in the Ordovician and sea level keeps falling throughout the Middle Ordovician. In contrast, Dronov (2004) suggests that there is a moderate regression at the base of the Volkhov Stage and that a prolonged highstand interval persisted during the Volkhov and Kunda stages, that reaches well into the Darriwilian Stage. Dronov (2004) and Artyushkov et al. (2008) argued that in northern Estonia sea level fluctuations rarely exceeded 20 m in amplitude.

The aim of this study is to analyse carbonate microfacies of limestone successions of the Pakri peninsula and outside the city of Tabasalu, west of Tallinn (Fig. 1). Based on detailed collection of rock samples and samples for stable carbon isotope analysis the general depositional evolution and changing bathymetry of the area has been evaluated. Sampling was conducted in several sections and the aim is to describe and compare these locations with respect to lithologies and relative sea level fluctuations.

## 2 Geological setting

Baltica (including the area of present-day Estonia) was located in the southern hemisphere during Ordovician times. The continent moved northward crossing different climate zones and at the end of the Ordovician, the Estonian region had reached a

subtropical position at 15-20° south of the Equator (Nielsen 2004; Nestor et al. 2007). Baltica was at that time surrounded by the Ural Ocean to the east (present-day direction), the Thornquist Sea to the southeast, and the Iapetus Ocean to the northwest (Cocks & Torsvik 2002; Cocks & Torsvik 2006). A vast epeiric sea covered most of the continent, now referred to as the Baltoscandian basin. This basin existed from the Neoproterozoic Ediacaran to Early Devonian time (Põldsaar & Ainsaar 2014). Due to late pre-Cambrian peneplanisation of the craton and little or no tectonic influence in the earliest Palaeozoic the basin was surrounded by low-relief landmasses of the Baltic Shield to the northeast and of the Ukrainian shield to the southeast (Kiipli et al. 2009).

The large scale facies distribution of the Baltoscandian basin is traditionally subdivided into confacies belts in which the sediments and benthic fauna reflect different water depths (e.g., Jaanusson 1976; Jaanusson & Bergström 1980). The Oslo and Scanian confacies belts are located in the deeper, western and southern parts of the basin, respectively, and mainly constitute graptolitic shales. The Central Baltoscandian Confacies Belt and the North Estonian Confacies Belt follows to the east (Fig. 1) and reflect intermediate and shallow-marine environments, respectively. These latter areas are therefore dominated by limestone facies. The belts also reflect a regional ecological zonation controlled by environmental factors (Jaanusson & Bergström 1980). An eastern extension of the Central Baltoscandian Confacies Belt is referred to as the Livonian Tongue. This slightly deeper embayment covered southern Estonia, the northwest of Latvia and western Lithuania. As a consequence, major lithological and facies differences between the north and south of Estonia are observed. Most of Estonia was part of the North Estonian Confacies Belt and was thus situated in a marginal area of the Baltoscandian basin with the inferred palaeoshoreline to the northeast. The total thickness of the Ordovician in Estonia varies from 70 – 180 m and is thickest in central and eastern Estonia (Meidla et al. 2014). The successions in the north of Estonia and the studied area are extremely condensed and many erosional surfaces reflect large gaps in the sedimentary record.

## 3 Stratigraphy of northern Estonia

Workers in the East Baltic area traditionally have used local to regional stages for the Ordovician, which have proved to be useful also in other countries of the Baltoscandic region. The relationship between regional and global Ordovician stages has more recently been outlined and defined by Bergström et al. (2009) and much of the recent improvements has been established in Estonia; see for example Nõlvak et al. (2006). Below follows a brief account of the regional Lower to Middle Ordovician stratigraphy concerned in this thesis with regard to chronostratigraphy, regional stages, lithostratigraphy and biostratigraphy. Figure 2 illustrates the relationships between series, stages, formations and conodont biostratigraphy. The chronostratigraphical classification used herein follows Berg-

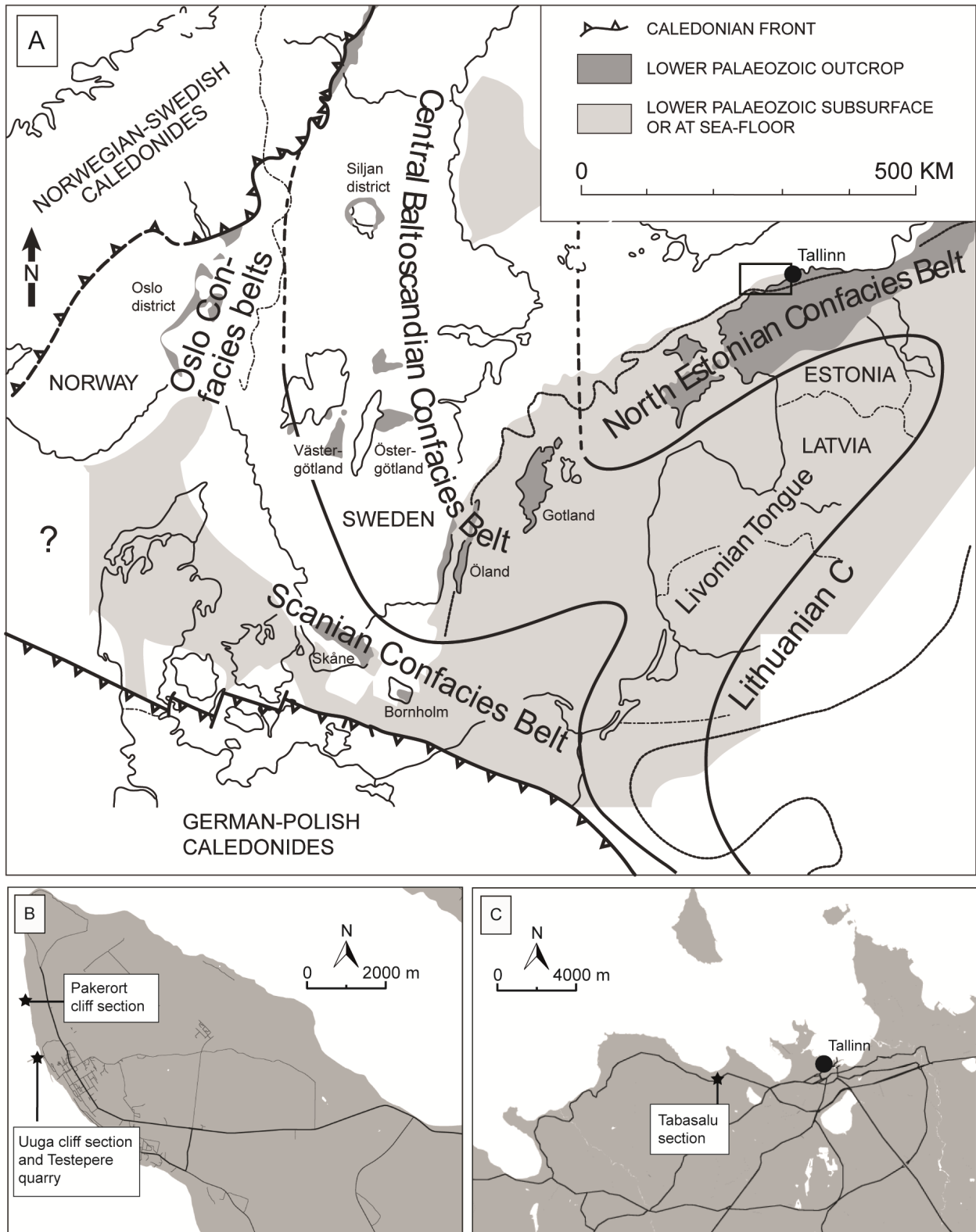


Fig. 1. Ordovician Paleogeography of Baltoscandia (above) modified from Nielsen (1995), facies belts modified from Jaanusson (1976, 1995). Pakri Peninsula (lower left) showing location of Pakerort cliff as well as Uuga cliff and the quarry outside Paldiski town. Tabasalu road cut section in relation to Tallinn (lower right). Square in Fig. 1A marks position of Figs. 1B and 1C.

ström et al. (2009), and the conodont biostratigraphy in Figure 2 is based on the zonation established by Viira et al. (2001), Löfgren et al. (2005), and Hints et al. (2012). For further sedimentary and biostratigraphy

work on the Pakri peninsula, see Löfgren et al. (2005). The lowermost Ordovician strata of northern Estonia belong to the Pakerort Stage. Lithostratigraphically they belong to the Turisalu Formation and consist of



Series	Global Stage	Balt. Stage	Conodont zones/ subzones	Formations in NW Estonia
Middle Ordovician	Darrivillian	Uhaku	<i>Baltoplacognathus robustus</i>	Kõrgekallas
		Lasnamägi	<i>Baltoplacognathus reclinator</i>	Vão
		Aseri	<i>Eoplacognathus foliaceus</i>	Aseri
		Kunda	<i>Eoplacognathus pseudoplanus</i>	Pakri
		Volkhov	<i>Paroistodus originalis</i>	Toila
Lower Ordovician	Floian	Billingen	<i>Baltoniodus navis</i>	Leetse
			<i>Oepikodus evae</i>	
	Tremadocian	Hunneberg	<i>Paroistodus proteus</i>	

Fig. 2. The Lower and Middle Ordovician stratigraphies of northwestern Estonia that are dealt with in this thesis (modified from Meidla & Ainsaar (2004)). Conodont zones according to Viira et al. (2001), Löfgren et al. (2005) and Hints et al. (2012).

kerogenous mudrocks. These are locally up to 7 m thick, become thicker towards the northwest coast of Estonia and are non-existent in the south (Raukas & Teedumäe 1997). The following Varangu Stage (corresponding to the Varangu Formation) deposits constitute a ca one-metre-thick suite of clay and silty sandstone with glauconite (Löfgren et al. 2005; Raukas & Teedumäe 1997).

The overlying strata belong to the Hunneberg

and Billingen stages. Hunneberg strata reaches up to 4 m in thickness in the northwest and is normally less than 2 m thick in south of Estonia (Raukas & Teedumäe 1997). These dark green, glauconitic sands and silts of the Leetse Formation are very loose, barely lithified and sometimes cross stratified. In central Estonia glauconitic sandstone have been deposited during the Billingen Stage while to the south reddish brown, and occasionally glauconitic dolomites occur

(Raukas & Teedumäe 1997).

The Volkhov Stage is represented by a main part of the Toila Formation and its partly dolomitized glauconitic limestone (Meidla et al. 1998). It is up to 4 m thick in north-western Estonia. The Volkhov Stage thickens considerably to the south where it reaches more than 20 m and is represented by the Kriukai Formation and its reddish marl, limestone and mudstone (Raukas & Teedumäe 1997).

The Kunda Stage is represented by the Pakri Formation and commonly consists of sandy limestone or calcareous sandstone with beds of conglomerate or breccia (Põldsäär & Ainsaar 2014). In the westernmost part of the country this stage is developed as a 4 m thick unit of nodular, kerogenous, calcareous sandstone. The stage thickens towards the south where it reaches more than 15 m and grades into the Rokiskis Formation (partly oolitic limestone) in central Estonia and Sakyna and Baldone formations in the very south (limestone containing glauconitic, clayey limestone respectively) (Raukas & Teedumäe 1997).

The Aseri Stage is represented by the Aseri Formation, a roughly 0.1-0.5 m thick unit composed of bioclastic limestone with goethitic ooids that are mostly brown to red in colour (Sturesson 1995). Ooids are normally frequent in this unit but in the dolomitic limestone of northeastern Estonia they occur only in the upper part of the formation (Raukas & Teedumäe 1997). In southern Estonia and the Central Baltoscandian Confacies Belt the Aseri Stage is represented by the Segerstad Formation, an up to 9 m thick limestone (Raukas & Teedumäe 1997).

The Lasnamägi Stage is represented by the Vão Formation, which is subdivided into three distinct members. A lower limestone with marly interbeds (Rebala Member) is overlain by a dolomite bed (the Pae Member) that is capped by a hard bioclastic limestone (Kostivere Member). The Vão Formation is previously described from the Uuga cliff section with regards to sedimentology as well as conodont (Hints et al. 2012) and chitinozoan biostratigraphy (Tammekänd et al. (2010)). The Vão Formation is between 4–10 m thick in Estonia and ranges into the Uhaku Stage (Raukas & Teedumäe 1997). In southern Estonia the Lasnamägi Stage is instead represented by micritic limestone of the Stirna Formation with a thickness up to 15 m (Raukas & Teedumäe 1997).

The early Uhaku Stage is represented by the hard bioclastic limestones of the upper Vão Formation and the slightly more argillaceous Kõrgekallas Formation in its younger parts. See Hints et al. (2012) for conodont stratigraphy and Tammekänd et al. (2010) for chitinozoan stratigraphy. The Uhaku Stage thickens considerably to the east of Estonia, from 5 to 25 m (Raukas & Teedumäe 1997).

## 4 Depositional cycles

Dronov & Holmer (1999) subdivided the Ordovician of Baltoscandia into a total of ten different third-order sea level cycles while others subsequently have divided the system into fourteen cycles (Dronov et al. 2011). This study treats the four of the cycles referred to as depositional sequence three through six of Dronov et al. (2011). A third order cycle normally

spans 0.5-10 My but is often shorter than 3 My (Plint et al. 1992). In Estonia the studied sequences represent 0.9-12 My (Dronov et al. 2011). It should be noted that not all depositional sequences are formed as a response to global sea level changes but may be responses to local tectonics and therefore also any combination of the two (Nichols 2009).

In the following chapters, the stratigraphy of the regional stages is described including the aspects of the studied localities. Regional stages correspond with depositional sequences and are described in ascending order as are the lithostratigraphical units described in each subchapter.

At the studied sections in the Pakri Peninsula, depositional sequence three through six (*sensu* Dronov et al. 2011) are exposed, whereas only sequence four through the lowermost part of sequence six crops out in the road-cut near Tabasalu. Depositional sequence three of Dronov et al. (2011) corresponds to the sand and silt sized glauconite of the Hunneberg Stage and the Billingen Stage with its greenish lime rich sand and siltstone that grades into a sandy limestone. Depositional sequence four of Dronov et al. (2011) corresponds to the Volkhov Stage and its grey limestone with glauconite. The lower boundary of the Volkhov Stage marks the base of a second order sea level cycle (Dronov & Holmer 1999) dominated by glauconitic limestone with marly interbeds and common hardgrounds. The base itself is a marked discontinuity surface known as “Püstakihit” in Estonia and “Blommiga bladet” in Sweden (Lindström 1979; Raukas & Teedumäe 1997; Ekdale & Bromley 2001) where it is a well-known hardground complex reflecting very low net sedimentation (Lindström 1963; Lindström 1979). Depositional sequence five of Dronov et al. (2011) corresponds to the Kunda Stage and a sandy limestone that grades upwards into a calcareous sandstone. The sixth depositional sequence of Dronov et al. (2011) corresponds to the local Aseri, Lasnamägi, and Uhaku stages. As a whole, these deposits formed in shallower environments than the underlying sequences four and five, probably by overall higher sedimentation rates.

## 5 Materials and methods

The field work for this study was conducted during five days in June of 2014. Among the studied localities are the Uuga cliff, Pakerort cliff, and Testepere quarry outside the town of Paldiski, as well as a road-cut along road 390 in Tabasalu (Fig. 1). The Uuga cliff and Tabasalu road-cut has been subject to rock sampling at roughly five-centimetre intervals. At these two locations whole rock  $\delta^{13}\text{C}$  samples for stable carbon isotope analysis were extracted using a hand-held micro-drill. Carbonate powders were subsequently reacted with 100% phosphoric acid ( $\text{H}_3\text{PO}_4$ ) at 70 °C with a Gasbench II connected to a ThermoFinnigan Five Plus mass spectrometer. All reported values are in per mil relative to Vienna Pee Dee Belemnite (V-PDB) by assigning  $\delta^{13}\text{C}$  and  $\delta^{18}\text{O}$  values of +1.95‰ and -2.20‰ to the international standard NBS19 and -46.6‰ and -26.7‰ to the international standard LSVEC, respectively. Reproducibility and accuracy of carbon isotope analyses were monitored by replicate

analysis of laboratory standards which were calibrated to NBS19 and LSVEC and were  $\pm 0.05\%$  ( $\pm 1$  std. dev.). In addition 37 rock samples were collected for preparation of thin sections. The samples were cut at the Institute of Geology at Tallinn University of Technology and sent to the University of Erlangen-Nürnberg where thin sections were prepared for microfacies analysis. The facies model from Harris et al. (2004) was used to link thin section microfacies to facies types (thus a marine environment) to describe sea level fluctuations of the Baltoscandian basin.

## 6 Sedimentary petrography of the Uuga cliff section and the Testepere quarry

The extensive outcrops along the west coast of Pakri peninsula (Fig. 3) have previously been studied by several authors (Löfgren et al. 2005; Tammekänd et al. 2010; Hints et al. 2012; Põldsaar & Ainsaar 2014). The three kilometres of continuous rock exposure, with strata dipping slightly towards the southeast, are easily accessed between the town of Paldiski and the tip of Pakri peninsula. Here the cliffs are steep and the cobble beach below is only a couple of metres wide. In the south, the cliff reaches a maximum of 10 meters in height, whereas towards the north, it is more than 20 meters high. The southern part of the escarpment, just outside of Paldiski, is referred to as the Uuga cliff section (Fig. 4, see also map in Fig. 1 for location) and exposes rocks of the Leetse Formation through the beginning of the Vão Formation. The abandoned Testepere limestone quarry is located in close proximity to this section (Fig. 5, see also map in Fig. 1 for location). In this quarry, the Vão Formation and the lowermost portion of the overlying the Kõrgekallas Formation has been quarried. Further north along the Pakri peninsula, successively more of the older units are exposed due to the dip of the strata to the south. The northernmost part of the escarpment is referred to as the Pakerort cliff and here even strata of early Cambrian age are exposed.

### 6.1 Toila Formation

The Toila Formation is 1.40 m thick at the Uuga cliff section and mainly constitutes a gray limestone with a wackestone to packstone texture. Glauconite is present throughout the Toila Formation but decreases upwards. Between 0.34 to 0.64 m above the base, the beds are slightly disturbed. Hardgrounds are most pronounced in the range of the 'Püstakkiht' hardground complex (basal 0.14 m) but also between 0.64 and 0.84 m above the base of the unit. In the latter interval, lenses of glauconitic marl increase. From 0.84 m towards the top of the formation large micritic clasts are common but pyrite concretions can also be seen. A few packstone and grainstone channels are also visible, roughly a few centimetres wide and a centimetre thick. Three samples were collected from the Toila Formation for microfacies analysis:

PAK-S-2: This thin section covers the interval between 0-0.14 m above the base of the Toila Formation (Fig. 6A). The interval displays the "Püstakkiht" hardground complex that consists of three hardgrounds within a vertical interval of 0.14 m. In the

bottom there is a bioclastic packstone with mainly trilobite and brachiopod fragments. Dark green glauconite grains are present but not abundant. Above this is a diffuse, brownish hardground with a thin mineralization and deep borings. Above the lowermost hardground there is a packstone of mainly trilobite fragments (a few of them up to five centimetres long), which is extremely abundant in glauconite. The matrix abruptly changes into a trilobite wacke- to packstone with black spots below the uppermost hardground. The uppermost hardground is abraded and shows distinct deep borings in multiple places. Both hardgrounds appear to be oxidized in and around the borings down to two millimetres below the top of the surface giving it a black colour and a rugged surface. Above the upper hardground glauconite is abundant but decreases up and away from the hardground. In the packstone above the hardgrounds the trilobites still dominate but echinoderms are common as well.

PAK-S-3: This thin section covers the interval between 0.37-0.48 m above the base of the Toila Formation (Fig. 6B). The bottom part of the interval is a packstone with dominantly trilobite- but also brachiopod- and echinoderm fragments. Glauconite grains are present but not abundant. A grainstone lens can be seen below the hardgrounds. At 0.05 m from the bottom of this interval is a brownish, bored and corroded hardground. The surface is clear-cut in places but more undulating in others. The hardground displays a fading mineralization from a dark brown to light brown, sometimes spanning as much as one centimetre. Black oxide spots are present but not common just underneath the hardground. Above the lowermost hardground there is yet another, more distinct, grainstone layer, a couple of millimetres thick. Glauconite grains are very common here. Apart from this the matrix contains dominantly trilobites but brachiopods are also very common. At eight centimetres above the base of the interval another more diffuse, brownish, corroded hardground is present and the thickness of the mineralization is only a couple of millimetres thick. Below it there is abundant glauconite and above it there are many larger trilobite- and brachiopod shells of up to a centimetre in size before it grades into a packstone. Above the upper hardground there is a packstone dominated by trilobites and brachiopods. In the topmost part there is abundant glauconite, however it is not as frequent as between the two hardgrounds.

PAK-S-4: This thin section covers the interval between 0.84-0.88 m above the base of the Toila Formation (Fig. 6C). The matrix is a trilobite- and brachiopod rich wackestone. Most striking are micritic and wackestone clasts. The clasts are subangular to subrounded and more densely packed in the bottom of the thin section. Both matrix and clasts contain glauconite. Quartz grains are also common in the basal part.

### 6.2 Pakri Formation

The Pakri Formation is 0.98 m thick at the Uuga cliff section and includes mainly bioclastic limestone but also dolomitized wackestone to packstone. The contact to the underlying Toila Formation is an unconformity. The lowermost part of the formation is strongly reworked and has a sugary, sandy texture. Several extensively bored hardgrounds are visible between 0.10-

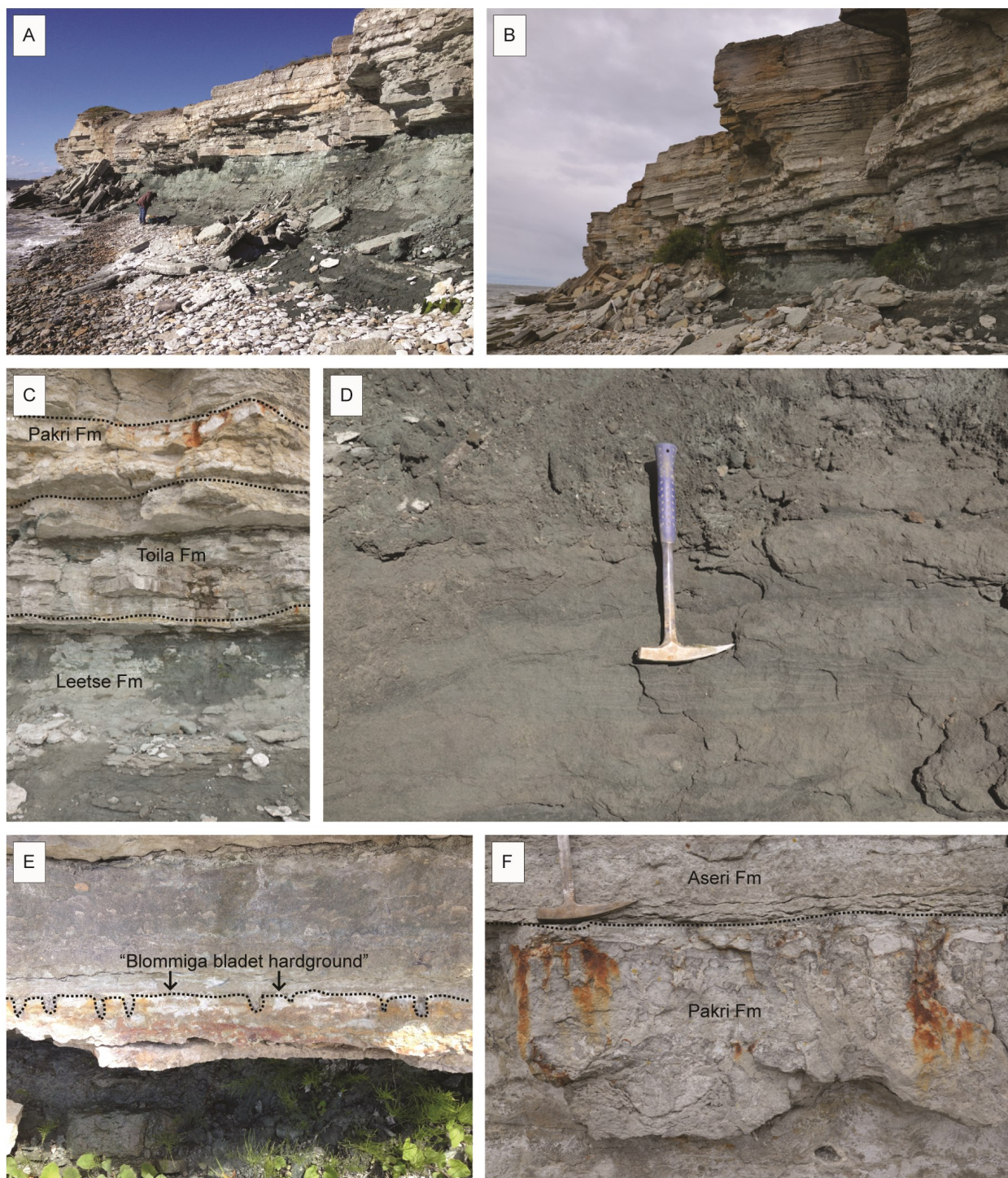


*Fig. 3.* Photographs of the Uuga cliff section. A. Top of the Leetse Formation through the Aseri Formation and beginning of the Vão Formation. B. Overview of the Leetse Formation through the Vão Formation. C. The Leetse Formation through Aseri Formation, reaching in to the Vão Formation. Note the gradual change from the (Leetse Formation to the Toila Formation) sandy limestone to limy sandstone. D. The Leetse Formation with its striking green glauconite sand and visible cross stratification. E. The Toila Formation with most notably the “Püstakkiht” hardground complex with its display of colours and deep borings. F. The Pakri Formation with cephalopod macrofossils and argillaceous limestone.

0.50 m above the base of the formation. In the top part of the Pakri Formation limestone clasts are present in a sandy matrix. The angular to subangular clasts are dolomitized wackestone most commonly between 0.02-0.03 m in size but they may range up to 0.30 m. Hardgrounds cut through the clasts. Higher up, the

Pakri Formation appears more disturbed and contains more inhomogenous brecciated limestone. There are grainstone and packstone channels but also glauconitic, marly lenses. The four thin sections from the Pakri Formation that have been examined for their petrographic characteristics are presented here.

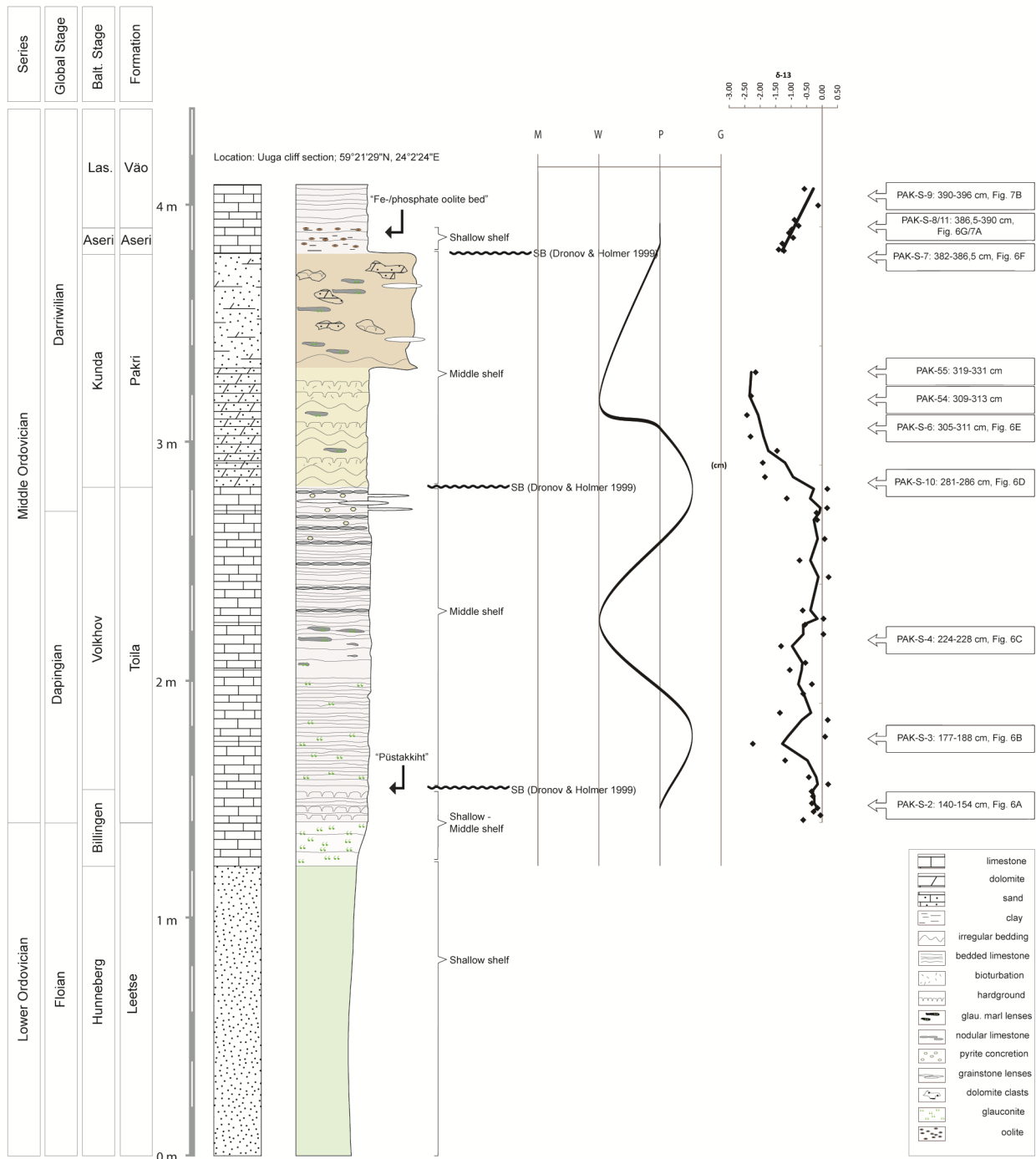


Fig. 4. Stratigraphy, sedimentary profile, carbonate microfacies, and carbon isotope chemostratigraphy of the Uuga cliff section. Thin sections sampled at regular intervals from the Toila through Aseri formations and lowermost Vão Formation. See separate Appendix 1 for exact sampling levels of stable carbon isotopes.

PAK-S-10: This thin section covers the interval between 0-0.05 m above the base of the Pakri Formation (Fig. 6D). The interval shows a calcareous sandstone with micritic mud between sand grains, appearing as solution seams. It also contains few shell fragments of brachiopods and trilobites. Sand-sized grains are subrounded to rounded quartz.

PAK-S-6: This thin section covers the interval between 0.24-0.30 m above the base of the Pakri Formation (Fig. 6E). This interval is strongly reworked. The matrix is a quartz-rich limestone to calcareous

sandstone. Quartz grains are sometimes of silt size and thus more angular in shape. The matrix has few but visible larger shell fragments (gastropods, echinoderms, trilobites, brachiopods) but also micritic lenses or clasts. Also in the matrix are rhombic dolomite crystals. One blackish hardground is visible at the base. Its mineralization varies in thickness, up to a millimetre at most, and is not recognizable in places. The surface is smooth but not flat and abraded. Borings are filled with light grey packstone that also seems to drape the hardground. At least two other,

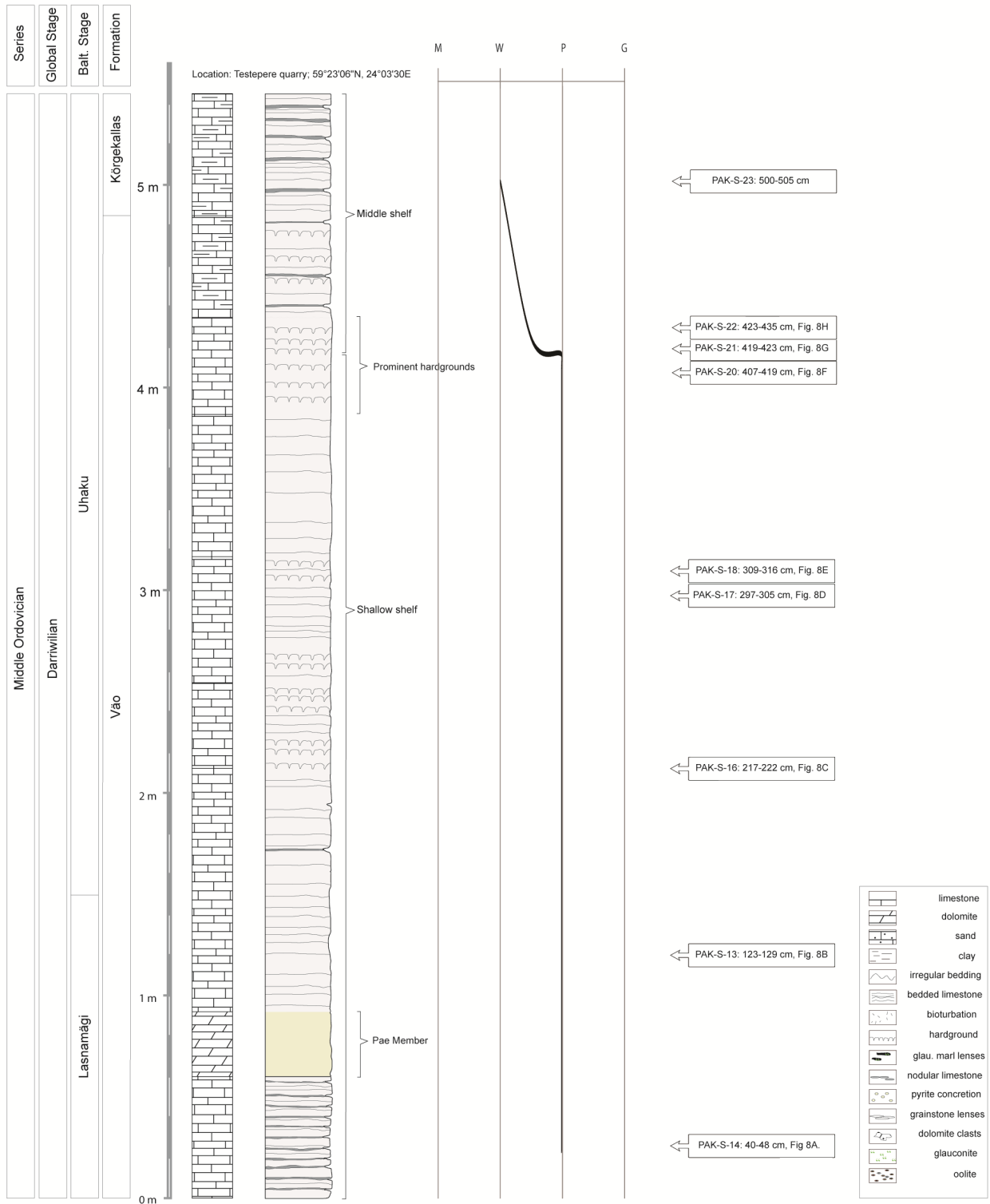


Fig. 5. Stratigraphy, sedimentary profile, and carbonate microfacies of the quarry outside of Paldiski. Thin sections sampled at regular intervals from the Vao Formation reaching into the Kõrgekallas Formation.

corrosional hardgrounds can be vaguely seen in the top part of the interval.

PAK-S-54: This thin section covers the interval between 0.28-0.32 m above the base of the Pakri Formation. The thin section has a horizontally layered appearance. The layers contain either sand- or packstone. Brown micrite- and wackestone clasts are also a

part of the layered appearance. These clasts are up to a couple of millimetres in diameter and rounded to subangular in character and contain glauconite. Mud solution seams can also be seen in the thin section, occasionally as dividing the sand grains from the packstone and clasts.

PAK-S-55: This thin section covers the interval

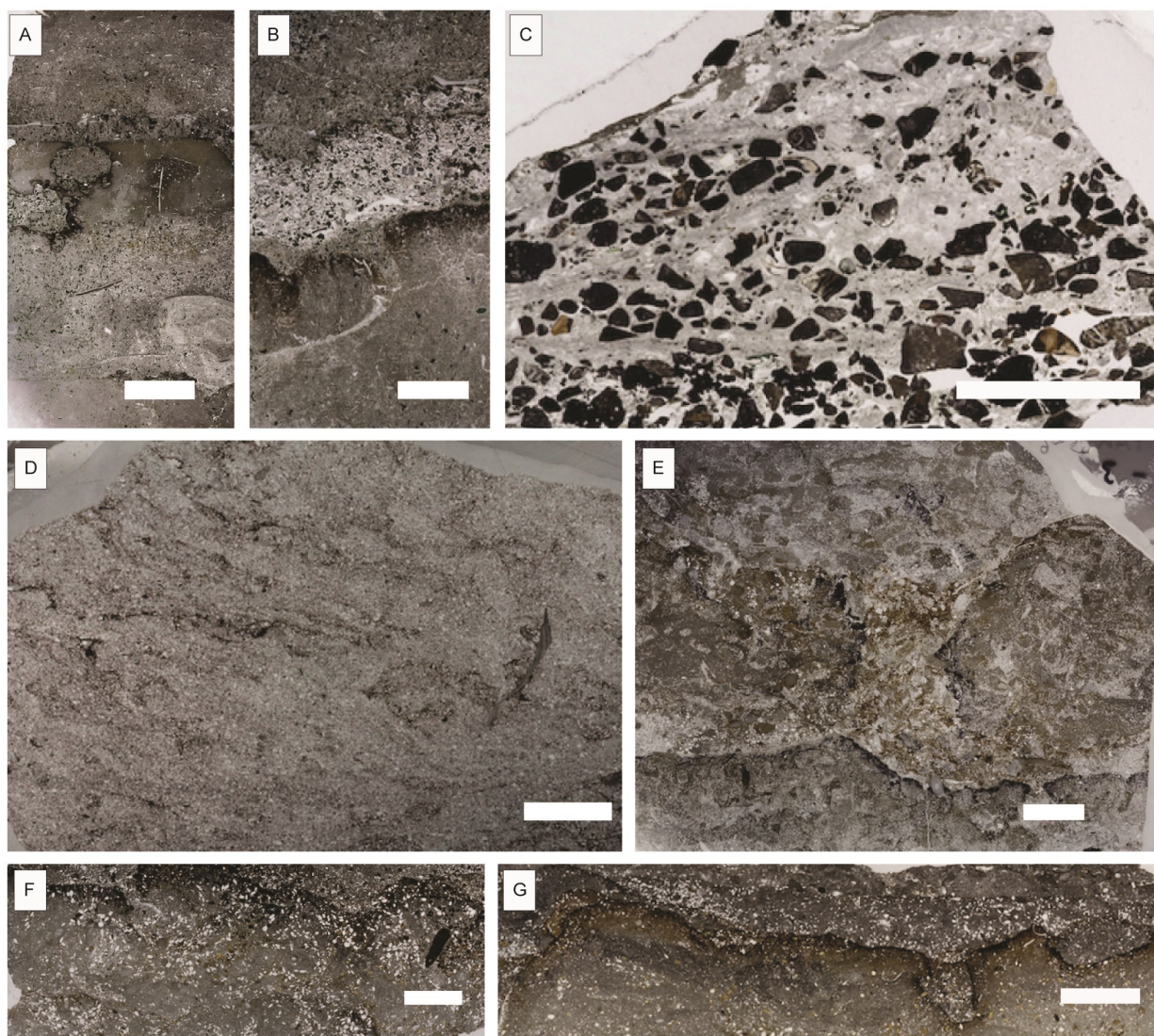


*Fig. 6.* Thin section micrographs of the Toila through Aseri formations from the Uuga cliff section. A. Displays the "Püstakkiht" hardground complex (Toila Formation). B. Packstone with a bored, corrosive hardground but also occasional grainstone lenses (Toila Formation). C. Wackestone with micritic and wackestone clasts that contain glauconite (Toila Formation). D. Limy sandstone with micrite mud and shell fragments (Pakri Formation). E. Strongly reworked thin section with several hardgrounds (Pakri Formation). F. In this thin section the top or bottom surfaces of hardgrounds are not very clear cut but stand out because of their thickness. Borings are occasionally subhorizontal (Aseri Formation). G. Packstone with mostly trilobite- and echinoderm fragments. Abundant red and brown ooids are seen and are clustered in the borings of hardgrounds (Aseri Formation). Scale bar is 1 cm in all photographs.

between 0.38-0.50 m above the base of the Pakri Formation. The bottom of the interval is a packstone and above a very sandy wackestone. The change is abrupt and can be traced through the whole width of the thin section. The packstone contains mostly trilobite- and echinoderm shell fragments but also gastropod fragments and scattered glauconite grains. The upper section (the sandy wackestone) is disturbed and reworked. Aside from an upwards increasing sand content it also shows brown micrite to wackestone clasts and occasional glauconite. The clasts are rounded to subangular.

### 6.3 Aseri Formation

The Aseri Formation in this section is only 0.11 m thick and constitutes clay-rich limestone with ooids.

The lower boundary and contact towards the Pakri Formation is an erosional unconformity. Ooids are brownish to reddish in colour. Three thin sections have been sampled for sedimentary petrography:

PAK-S-7: This thin section covers the interval between 0.035-0.07 m above the base of the Aseri Formation (Fig. 6F). The thin section has abundant red and brown ooids (or moulds displayed by empty ellipses) of about one or two millimetres in diameter. The ooids do not seem to be randomly scattered. They are rather clustered in borings of hardgrounds and other pockets. Largely the matrix is a muddy packstone with shell fragments mostly from trilobites and echinoderms in equal proportion but also brachiopods are present. At least two hardgrounds are seen in the top of the interval where they partly converge into one. The

colour is dark brown to black. The hardgrounds surface is not very clear-cut but instead stand out because of the thickness of its mineralization, sometimes more than one centimetre. Borings are up to a centimetre deep and occasionally horizontal.

PAK-S-8: This thin section covers the interval between 0.07-0.11 m above the base of the Aseri Formation (Fig. 6G). The matrix is a packstone with mostly trilobite- and echinoderm fragments. Abundant red and brown ooids (sometimes moulds) are seen and are clustered in the borings of hardgrounds. There are at least four different hardgrounds that sometimes merge and make up fewer but thicker mineralizations. The mineralizations differ in development but are all dark brown fading into the grey colour of the matrix of the underlying limestone and no more than a couple of millimetres thick at most.

PAK-S-11: This thin section covers the interval between 0.07-0.11 m above the base of the Aseri Formation (Fig. 7A). The interval contains a packstone with abundant trilobite-, brachiopod-, and echinoderm shell fragments. Mud seams are present in the lower part of the thin section. Ooids are present throughout the whole interval but increase upwards and seem to have more of a random scattering. Two brown hardgrounds appear in the middle of this interval. The mineralizations are brownish in colour, corroded and a couple of millimetres thick. The surface is smooth and fades in brown colour from dark to lighter.

## 6.4 Vão Formation

Only the basal 0.18 m of the Vão Formation is exposed in the topmost part of the Uga cliff section. At the Testepere quarry located a few hundred metres east from the cliff, a 4.85 m thick section of the Vão Formation has been measured instead. Here it can be subdivided into three distinct members. Limestone with marly interbeds at the bottom is overlain by a dolomite bed (the Pae Member) that is 0.32 metres thick. It is capped by a hard bioclastic limestone of mostly packstone character. Hardgrounds are common and between 2.12-2.54 m above the base of the Vão Formation six distinct hardgrounds are visible. Higher up, between 4.15-4.35 m above the base, another set of six hardgrounds is visible. Between 3.17 and 3.87 m above the base, there are also small lenses of grainstone. Nine samples have been collected and studied in thin sections.

PAK-S-9: This thin section covers the interval between 0-0.06 m above the base of the Vão Formation (Fig. 7B) and constitutes a trilobite packstone that contains gastropods and echinoderms. Ooids are present in the whole thin section but clearly decrease or almost disappear above the most distinct brown hardground. Quartz sand grains are scattered in the whole thin section but have accumulated above the aforementioned hardground.

PAK-S-14: This thin section covers the interval between 0.40-0.48 m above the base of the Vão Formation at the Testepere quarry (Fig. 8A). This interval is a light to dark grey packstone, mostly containing trilobites but also bryozoa and echinoderm fragments. Multiple stylolites can be seen in the interval but seem more common around the very bottom and the middle three to four centimetres of the interval.

PAK-S-13: This thin section covers the interval between 1.23-1.29 m above the base of the Vão Formation at the Testepere quarry (Fig. 8B). This is a packstone with mainly trilobite-, echinoderm- and bryozoa fragments. Beneath three vague hardgrounds there are mud solution seams. The hardgrounds show mineralization of brownish colour and they are visible towards the bottom where they also converge in places. The mineralizations are less than a millimetre thick and have smooth top and bottom surfaces.

PAK-S-16: This thin section covers the interval between 2.17-2.22 m above the base of the Vão Formation at the Testepere quarry (Fig. 8C). The interval consists of a bioclastic packstone containing mainly trilobite and echinoderm fragments, some larger than five millimetres in length. Accumulations of the larger shell fragments seem to be concentrated in pockets of hardground borings. A few mud solution seams can be seen across the very bottom of the interval. Four distinct hardgrounds are visible in this interval in upper part and sometimes merge. Borings are frequent, narrow and deep in the upper part. Some of the borings are horizontal. The hardgrounds are otherwise brownish to black and very sharp. The uppermost and most distinct hardground has a flat-topped surface.

PAK-S-17: This thin section covers the interval between 2.97-3.05 m above the base of the Vão Formation of the Testepere quarry (Fig. 8D). The interval contains a packstone with dominantly trilobites and echinoderms. The larger fragments seem to cluster in borings of hardgrounds. In the lower part of this interval there are also mud solution seams and the packstone has a darker grey appearance. Two developed hardgrounds are seen in the middle of this interval and converge into one in places.

PAK-S-18: This thin section covers the interval between 3.09-3.16 m above the base of the Vão Formation in the Testepere quarry (Fig. 8E). The bioclastic packstone contains fragments of bryozoans, echinoderms, and brachiopods. Two hardgrounds of different character are seen in this interval. The lower one is abraded, with a sharp mineralized surface. It shows deep and wide borings. The upper hardground is brownish, abraded and without borings.

PAK-S-20: This thin section covers the interval between 4.07-4.19 m above the base of the Vão Formation at the Testepere quarry (Fig. 8F). It is a packstone with abundant echinoderm-, brachiopod-, and trilobite fragments. Larger shell fragments are concentrated, but not exclusive to, the deeper borings. At least four different hardgrounds are identified in this interval. The upper- and lowermost are corroded, with very thin but distinct mineralizations of black colour and extensively bored. Borings are several centimetres deep and very narrow. Occasionally the borings are subhorizontal. The two hardgrounds in the middle are mostly converging into one but are distinctly separate in places. The mineralization colour is brownish and the top and bottom surfaces are clear-cut and abraded for the most part. Even when converging the hardgrounds are very thin, making up a millimetre in thickness at most.

PAK-S-21: This thin section covers the interval between 4.19-4.23 m above the base of the Vão Formation at the Testepere quarry (Fig. 8G). Echinoderm-



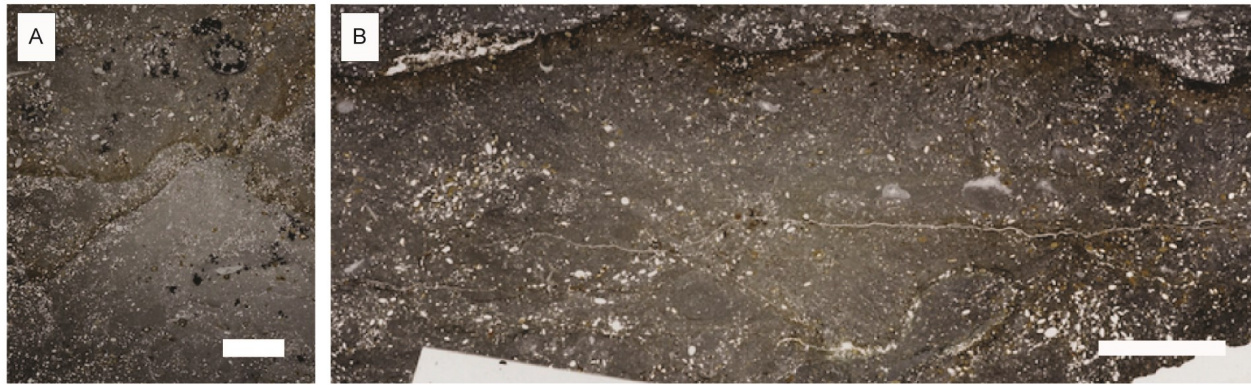


Fig. 7. Thin section micrographs of the Aseri and Vão formations from the Uuga cliff section. A. Packstone where ooids are present throughout the whole thin section but increase upwards (Aseri Formation). B. In this thin section ooids are present in the whole thin section but clearly decreases upwards (Vão Formation). Scale bar is 1 cm in both photographs.

and trilobite shell fragments make up most of this packstone but gastropods are also found. One black distinct and narrow hardground is seen in this interval. It is black and corroded, although not entirely flat-topped but with a rugged surface. Some wider and shallow borings occur. Some mud solution seams can be seen above the hardground but a few are also visible below.

PAK-S-22: This thin section covers the interval between 4.23-4.35 m above the base of the Vão Formation at the Testepere quarry (Fig. 8H). It is a wackestone to packstone with abundant trilobite- and echinoderm fragments but also some brachiopod- and bryozoa fragments. Shell fragment of centimetre size in diameter are found scattered around this interval. The interval contains at least four hardgrounds. It is extensively bored and sometimes one is difficult to distinguish from the next as they merge into each other and become part of the same hardground. The top and bottom ones are of abraded type and the two middle ones are corroded. The mineralizations are mostly very thin but distinct and black to brown in colour. In places the mineralizations grow more than a millimetre thick. The bottom hardground has shallow borings while the topmost has extremely deep (up to four centimetres) borings.

## 6.5 Kõrgekallas Formation

The Kõrgekallas Formation in this section is only 0.60 m thick in the topmost part of the Testepere quarry. It consists of a limestone of mostly wackestone with marly interbeds. One sample has been collected and studied in thin sections. PAK-S-23: This thin section covers the interval between 0.15-0.20 m above the base of the Kõrgekallas Formation at the Testepere quarry. It is a wackestone with brachiopods and trilobite fragments mostly. Many fragments are several millimetres or larger in size. The colour of the thin section is dark grey in the bottom and top few centimetres while the middle section is slightly lighter in colour. Mud solution seams can be seen across this interval.

## 7 Sedimentary petrography of the Tabasalu road cut section

The Tabasalu road-cut (Fig. 9) is situated along road

390 in the town of Tabasalu. It constitutes Middle Ordovician rocks belonging to the Toila Formation through the lower part of the Vão Formation. The exposure is 5.50 meters high (Fig. 10) and only a narrow bicycle track separates it from road 390 to Tallinn. Figure 14 illustrates stratigraphic levels in relation to the Uuga cliff section.

### 7.1 Toila Formation

The Toila Formation is 1.38 m thick at the Tabasalu road-cut and consists mostly of thin bedded limestone with a packstone texture. The formation has marly interbeds throughout its entire thickness although the thickness and frequency of the marly beds increase upwards. Glauconite is present and increases upwards. Four thin sections have been sampled and are presented below.

KAL-S-3: This thin section covers the interval between 0.25-0.32 m above the base of the Toila Formation (Fig. 11A). The matrix is an echinoderm- and trilobite rich packstone but it also contains much larger shell fragments, up to several millimetres across. Glauconite is common throughout the whole section. At two levels in the thin section a very distinct colour shift takes place from grey to brown. Several millimetres in thickness it resembles a ripped-up, corroded hardground.

KAL-S-7: This thin section covers the interval between 0.70-0.73 m above the base of the Toila Formation (Fig. 11B). The matrix is a trilobite- and echinoderm rich packstone. Mud solution seams are abundant across the interval. In places the mud seams are densely packed and taken together they are one millimetre or more in thickness. Glauconite is common and seems to be concentrated in, but is not exclusive to, the darker grey packstone. The lighter grey areas of the interval on the other hand contains larger shell fragment, sometimes several millimetres in length.

KAL-S-10: This thin section covers the interval between 1.20-1.25 m above the base of the Toila Formation (Fig. 11C). The interval displays a gradual colour change from a dark grey to brownish colour in the bottom towards a light grey at the top. The matrix is a packstone dominated by trilobites. Sand grains can be spotted in the whole thin section, often close to more or less developed mud seams and a darker grey colour,

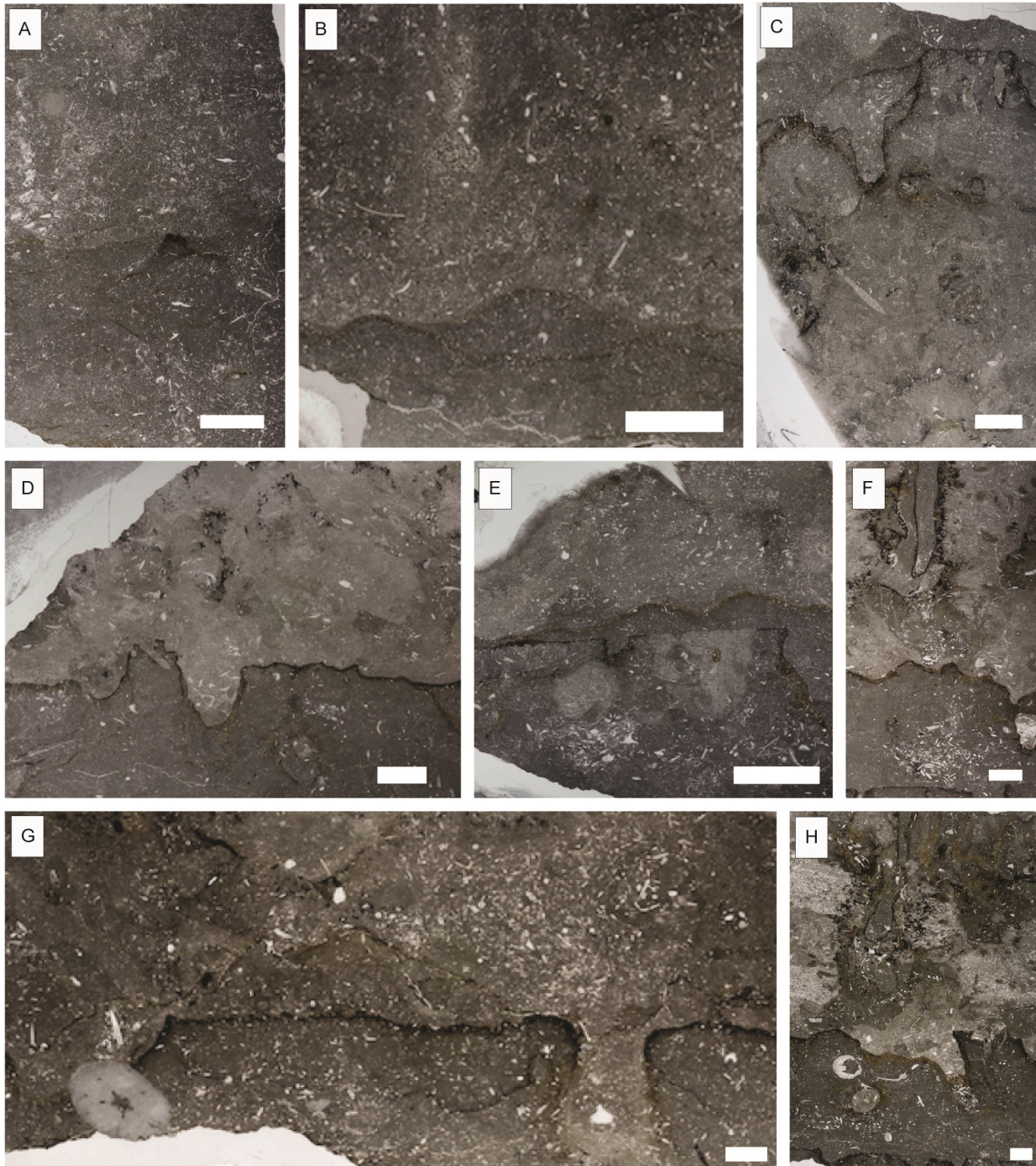


*Fig. 8.* Thin section micrographs of the Vão Formation from the Uuga cliff section. A. Packstone with multiple mud solution seams across the entire thin section (Vão Formation). B. Hardgrounds with smooth top and bottom surfaces (Vão Formation). C. Four distinct hardgrounds. Borings are frequent (Vão Formation). D. Hardgrounds that show clear-cut top and bottom surfaces. Borings are deep, narrow and subhorizontal (Vão Formation). E. Deep and wide borings in lower hardground. Upper hardground is less clear-cut in both upper and lower surface and without borings (Vão Formation). F. At least four different hardgrounds. The uppermost and lowermost are corroded and extensively bored. Borings are several centimetres deep and very narrow. Occasionally the borings are horizontal appearing as a hole in the thin section. G. Distinct corroded and narrow hardground. Some wider and shallow borings occur (Vão Formation). H. At least four different hardgrounds, extensively bored. The bottom hardground has shallow borings while the topmost has extremely deep (4 cm) borings. The bottom half of the thin section is a packstone and the top is a wackestone. Scale bar is 1 cm in all photographs.

but are mostly concentrated to the bottom few centimetres. Glauconite is common throughout the interval but gradually increases upwards where it is abundant.

KAL-S-12: This thin section covers the interval between 1.32-1.38 m above the base of the Toila Formation (Fig. 11D). The bottom matrix shows a trilo-

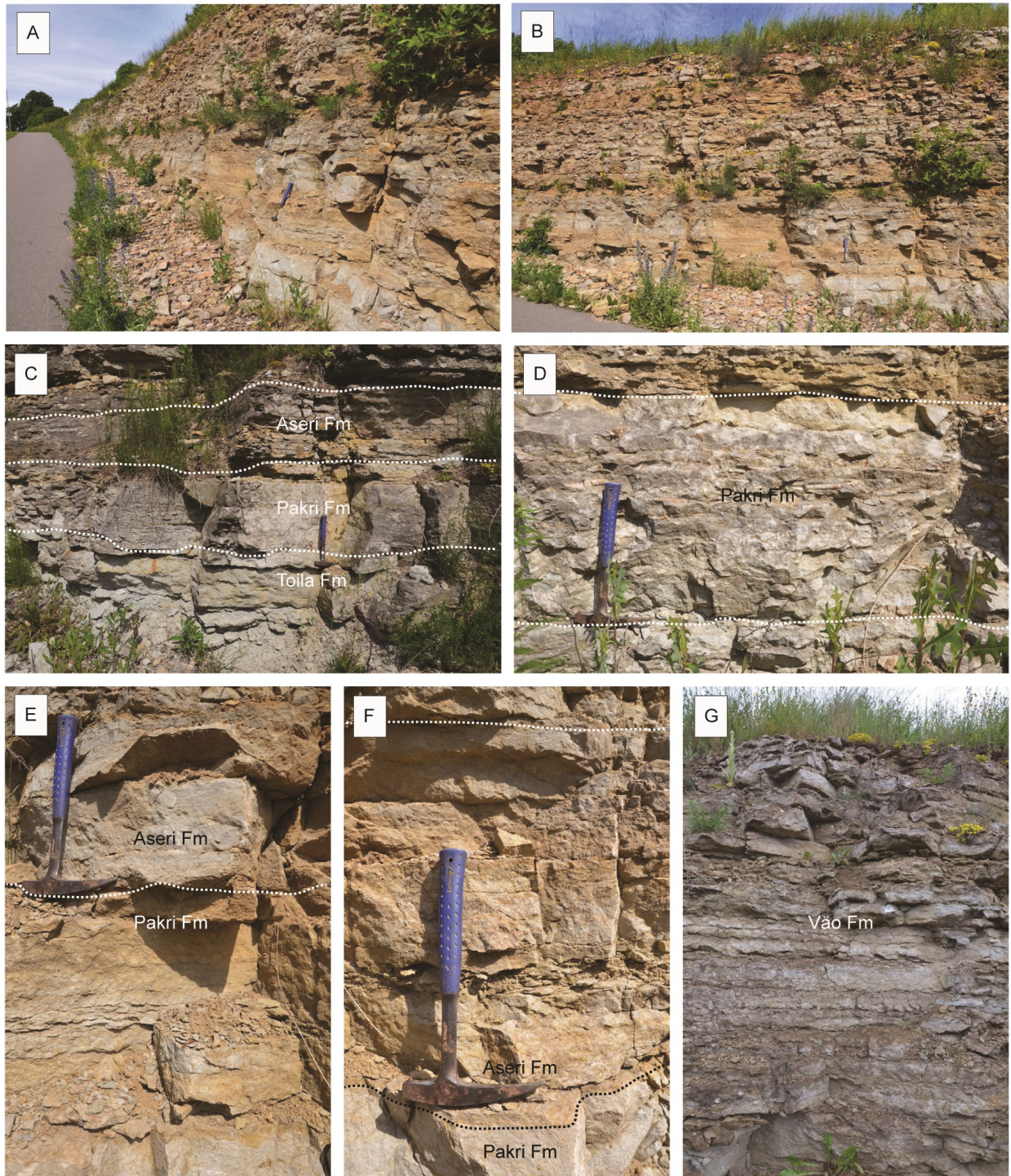


*Fig. 9.* Photographs of road cut section outside the town of Tabasalu. A-B. Overview of section showing the lithology from the Toila Formation to the Vão Formation. C. The Massive ledge of the Pakri Formation is displayed with its brownish spots of ooids. The upper part of the photo shows a more argillaceous Aseri Formation and beginning of the Vão Formation. D. Pakri Formation close-up with cephalopod macrofossils. Some brown ooids of the “Lower oolite bed” and “Upper oolite bed” can be seen. E. Top of the Pakri Formation and the whole Aseri Formation indicating the three different oolite beds, “Lower oolite bed” and “Upper oolite bed” of the Pakri Formation, but also the Aseri Formations reddish ooids F. Close-up of the Aseri Formation also showing the boundary between the Pakri Formation and Aseri Formation from a grey to reddish colour of the limestone. G. The Vão Formation with its argillaceous interbeds.

bite dominated packstone that also contains a very visible and well preserved gastropod shell, more than two centimetres long. Glauconite is abundant in this section and evenly spread. Above this there is a

hardground with a mineralization of black colour. The matrix above this hardground shows a trilobite- and echinoderm dominated packstone. Patches of larger shell fragment (more than one centimetre across) ap-

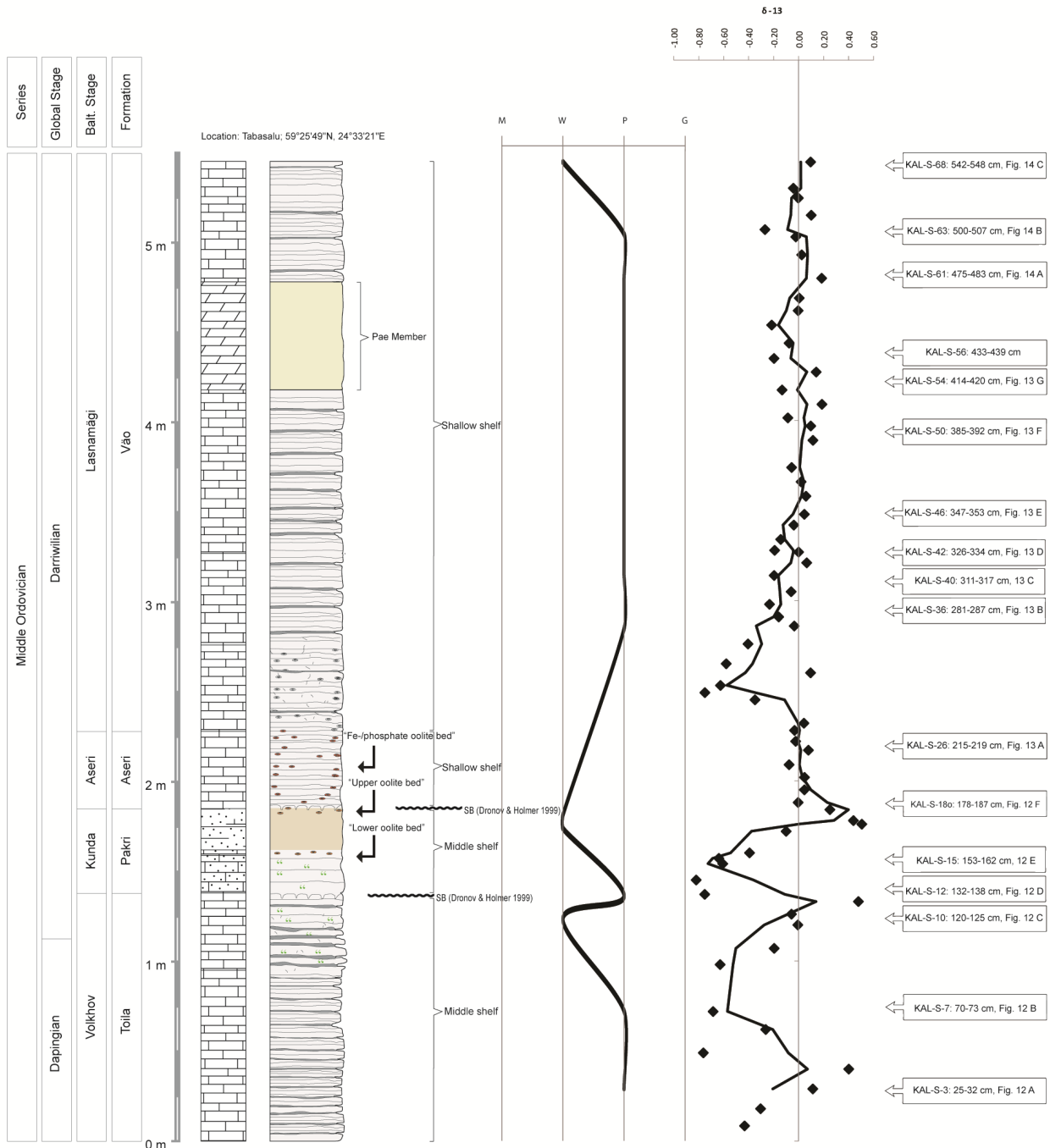


Fig. 10. Stratigraphy, sedimentary profile, carbonate microfacies, and carbon isotope chemostratigraphy of the road cut section outside the town of Tabasalu. The changes in local depositional depth are based on a general carbonate microfacies analysis of thin sections. Thin sections sampled at regular intervals throughout the profile. See separate Appendix 1 for exact sampling levels of stable carbon isotopes.

pear and seem to be concentrated where the hardground mineralizations are at its thinnest or where it is discontinuous. This part of the matrix is extremely abundant in glauconite grains. The second and uppermost hardground of this interval has a distinctly cut top surface. In most places it is very thin but sometimes reaches up to two millimetres in thickness. A few borings can be seen but they are small, up to five millimetres deep. The matrix above this hardground is very sandy brownish to grey wackestone.

## 7.2 Pakri Formation

The Pakri Formation in the Tabasalu road-cut is 0.47 m thick and is partly silicified in the lowermost part. It constitutes a limestone with a packstone texture, that up-section is transitional to a calcareous sandstone, and two distinct layers contain ooids of brown to red color. The formation contains both large cephalopods and gastropods well visible in the outcrop.

KAL-S-15: This thin section covers the interval between 0.15-0.24 m above the base of the Pakri Formation (Fig. 11E). The matrix is a dark grey packstone

throughout the interval. It contains trilobite- and echinoderm fragments but also occasional gastropod fragments. Glauconite is abundant in the lowermost part. There are two hardgrounds in the middle of this interval of which the lowermost has brownish mineralization and borings that are up to a few centimetres deep. Above this hardground glauconite becomes less common and two centimetres above it there is another hardground of similar character only without the borings. Above the second hardground glauconite is more common again. Abundant ooids are found in the top half of the interval but is largely missing below the lowermost hardground.

KAL-S-18o: This thin section covers the interval between 0.40 m above the base of the Pakri Formation to 0.02 m above the base of the overlying Aseri Formation, i.e. the boundary interval (Fig. 11F). The lowermost part displays a sandy packstone containing dominantly trilobite shell fragments. This lower part also contains mud solution seams. Glauconite grains are very common and seem randomly distributed. A dark brownish hardground, with its mineralization a couple of millimetres thick, separates two distinctly different lithologies. The brownish colouration extends down and gradually fades in colour until another, discontinuous hardground appears. Above the upper hardground is a sandy wackestone with mainly trilobite- and echinoderm fragments. It is also rich in brown ooids.

### 7.3 Aseri Formation

The Aseri Formation is 0.43 m thick and constitutes a thin bedded packstone. The most striking feature of the unit is the red ooids that appear in the whole formation. One sample has been collected for analysis of sediment petrography.

KAL-S-26: This thin section covers the interval between 0.30-0.34 m above the base of the Aseri Formation (Fig. 12A). The interval is extremely rich in ooids and also contains some quartz sand grains in a wacke- to packstone matrix. At least two corroded hardgrounds appear with smooth dark brown mineralized surfaces several millimetres thick in places. Both hardgrounds are bored and in these borings the hardgrounds are discontinuous.

### 7.4 Vão Formation

The Vão formation has a thickness of 3.17 m and is composed of limestone with argillaceous interbeds that increase somewhat in frequency and thickness upwards. The limestone is mostly of packstone character. There is a light brown dolomite layer (the Pae member) that is 0.60 m thick between 1.90-2.50 m in the measured section. Above the Pae Member there is much less or no argillaceous material. Ten thin sections have been sampled for analysis of sediment petrography and are presented here.

KAL-S-36: This thin section covers the interval between 0.53-0.59 m above the base of the Vão Formation (Fig. 12B). This is a packstone containing mostly trilobite- and brachiopod shell fragments. In the lower part of the interval there is a brownish packstone that contains vertical bands of dolomitized limestone from the bottom and up. In the middle and upper part of this interval there are patches of calcite cement.

KAL-S-40: This thin section covers the interval between 0.83-0.89 m above the base of the Vão Formation (Fig. 12C). This is a dark grey to brownish muddy packstone where mud content increases upwards. It is also dolomitized in the upper part of the interval and further contains patches of calcite cement scattered in the whole section. The top part also contains multiple mud solution seams of which some converge into a package reaching almost a millimetre in thickness.

KAL-S-42: This thin section covers the interval between 0.98-1.01 m above the base of the Vão Formation (Fig. 12D). Brownish wacke- to packstone of dominantly trilobite fragments. It contains brownish colouration from mud content.

KAL-S-46: This thin section covers the interval between 1.19-1.25 m above the base of the Vão Formation (Fig. 12E). This is a packstone with dominantly trilobite fragments. Some calcite cement is present and also dolomitization in places. The colour is light grey but the high mud content gives this interval a brownish appearance.

KAL-S-50: This thin section covers the interval between 1.57-1.64 m above the base of the Vão Formation (Fig. 12F). It is a trilobite rich brownish packstone with occasional dolomitization. Some patches contain calcite cement. This interval is muddy and also contains a few mud solution seams.

KAL-S-54: This thin section covers the interval between 1.86-1.92 m above the base of the Vão Formation (Fig. 12G). This is a trilobite rich packstone containing slightly larger shell fragments in the lower part of the interval. The upper part on the other hand seems more affected by dolomitization, but also contains more silt sized quartz grains and a few mud solution seams.

KAL-S-56: This thin section covers the interval between 2.05-2.14 m above the base of the Vão Formation. A brownish packstone with mainly trilobite- and echinoderm fragments but also bryozoa fragments visible. This packstone is muddy and dolomitization is showing in some places.

KAL-S-61: This thin section covers the interval between 2.47-2.55 m above the base of the Vão Formation (Fig. 13A). Echinoderm- and larger brachiopod fragments are common in this brownish packstone. Muddy patches can be seen in the lower part of the interval while in the middle and upper part there is a complex pattern of mud solution seams and also dolomite.

KAL-S-63: This thin section covers the interval between 2.72-2.79 m above the base of the Vão Formation (Fig. 13B). Patches of calcite cement throughout a brownish thin section that otherwise contains a packstone of dominantly trilobite- and echinoderm fragments. Several mud solution seams are seen across this interval. Gastropod- and bryozoa fragments are visible.

KAL-S-68: This thin section covers the interval between 3.14-3.20 m above the base of the Vão Formation (Fig. 13C). This is a trilobite- and echinoderm (gastropods are also recognized) rich wackestone. The interval has a thick mud solution seam of dark brown colour across the middle part. Mud is present in the interval but not dominant anywhere. Dolomitization is

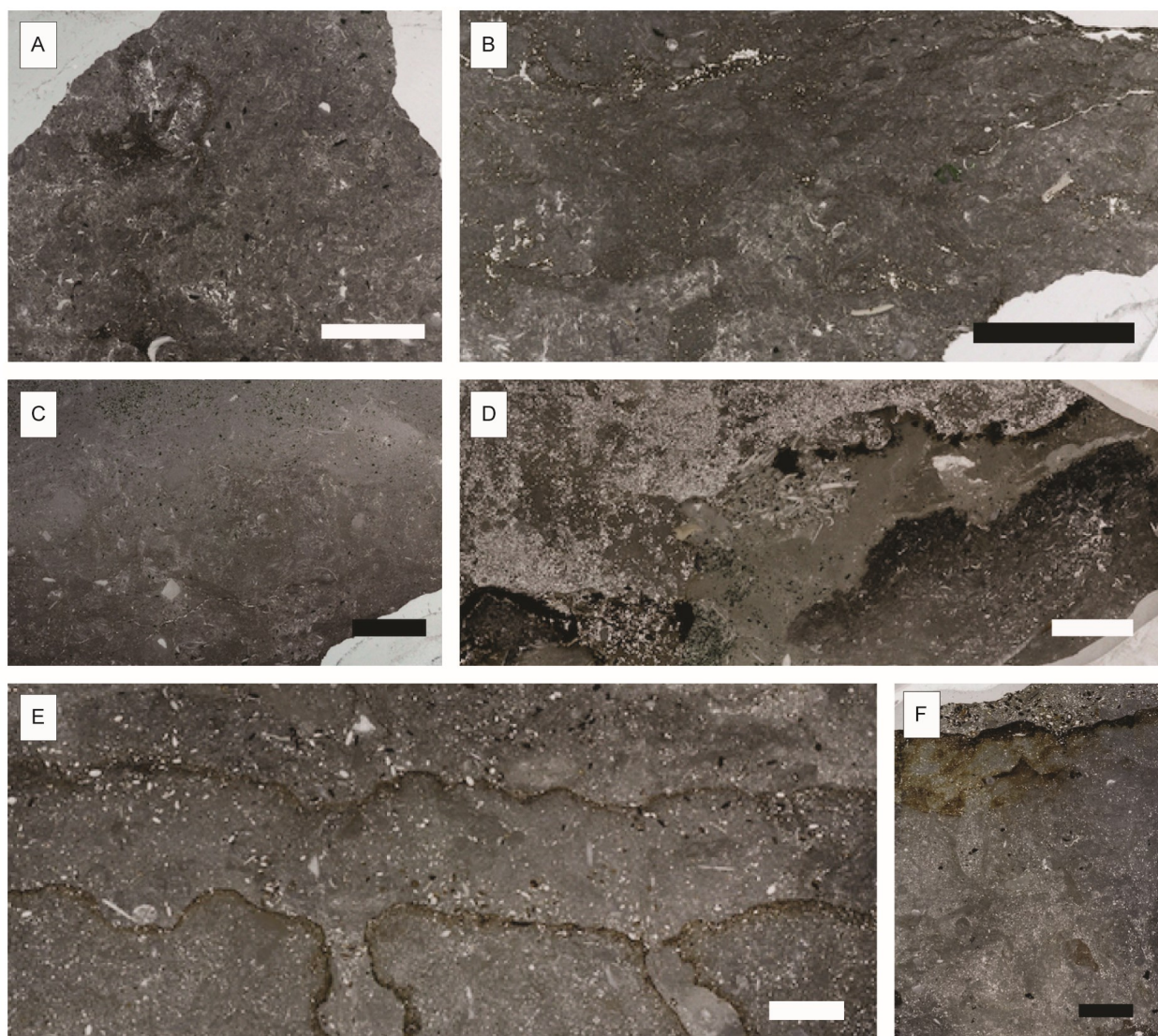


*Fig. 11.* Thin section micrographs of the Toila through Aseri formations from the Tabasalu road cut section. A. The matrix is a packstone and glauconite is common across the whole section (Toila Formation). B. The matrix is a packstone. Glauconite is common and seems to be concentrated in, but is not exclusive to, the darker grey packstone (Toila Formation). C. Packstone where glauconite is very common throughout the thin section but gradually increases upwards (Toila Formation). D. Two hardgrounds separate the thin section into three different lithologies. Borings can be seen in the upper hardground, up to five millimetres deep. The bottom matrix shows a packstone. Glauconite is abundant. The matrix in the middle shows a packstone that is extremely abundant in glauconite grains that also seem to be concentrated in patches. The uppermost matrix part is a very sandy brownish to grey wackestone (Toila Formation). E. Two brownish hardgrounds, both are abraded and the lower one has borings, up to a few centimetres deep. The matrix is a packstone. Abundant ooids are found in the top two sections. Glauconite is abundant in the bottom and top part (Pakri Formation). F. Hardground separates two distinctly different lithologies. Below is a sandy packstone. Glauconite grains are very common. Above is a sandy wackestone with mainly trilobite- and echinoderm fragments. It is also rich in brown ooids (Aseri Formation). Scale bar is 1 cm in all photographs.

visible and mostly shows below the mud seam.

## 8 Stable carbon isotope data

Previous measurements of  $\delta^{13}\text{C}$  have been carried out in the Aseri Formation through the Vão Formation at the Uuga cliff by Tammekänd et al. (2010). For further information on  $\delta^{13}\text{C}$  stable carbon isotope measurements in the Ordovician of Estonia see Kaljo et al. (2007) and references therein.

Samples for stable carbon isotope analysis were collected at the Uuga cliff section, ranging from the Toila Formation to the lower part of the Vão Formation,

with the exception for the upper Pakri Formation. In the Tabasalu road-cut section samples were collected between the Pakri and Vão formations. The  $\delta^{13}\text{C}$  data from the Uuga cliff (Fig. 4) shows values between -2.43‰ and 0.21‰. The Pakri Formation stands out with exceptionally low values, between -1.45‰ to -2.43‰. Otherwise the variations are very small, varying between 0‰ and -1‰ for the most part. The  $\delta^{13}\text{C}$  stable carbon isotope curve of the Tabasalu road-cut (Fig. 10) on the other hand shows variations between -0.82‰ and 0.51‰. A slight but steady increase can be seen from the lower portion of the Vão For-

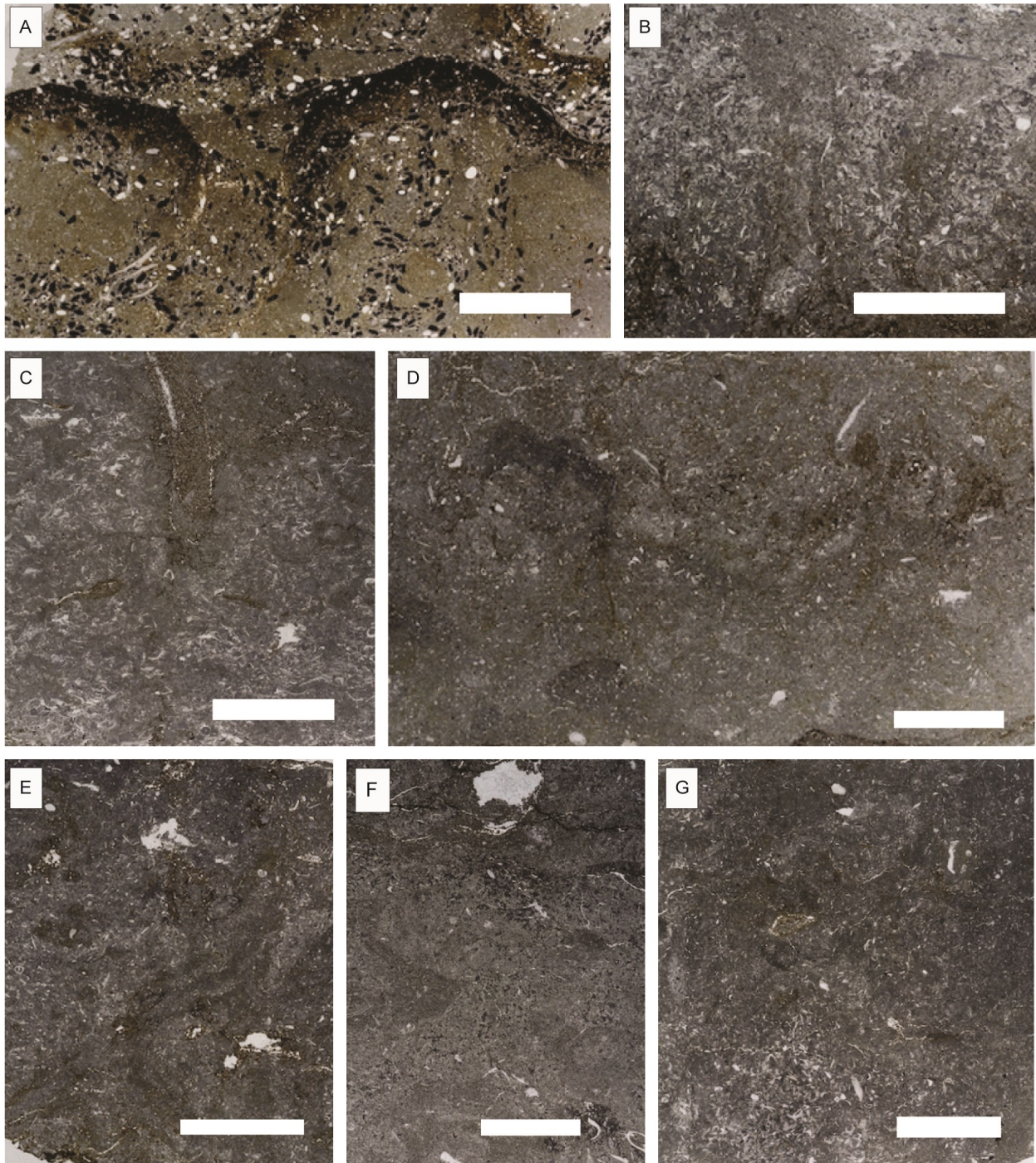


*Fig. 12.* Thin section micrographs of the Aseri and Vão formations from the Tabasalu road cut section. *A.* Two corroded and bored hardgrounds. Extremely ooid rich and also contains quartz sand grains in a wacke- to packstone matrix (Aseri Formation). *B.* A packstone with mostly trilobite- and brachiopod fragments (Vão Formation). *C.* A muddy packstone where the mud content increases upwards (Vão Formation). *D.* Trilobite rich wacke- to packstone (Vão Formation). *E.* Trilobite packstone. Calcite cement is present and also areas of dolomitization. High mud content gives the whole thin section a brownish appearance (Vão Formation). *F.* This thin section shows a trilobite rich packstone (Vão Formation). *G.* Trilobite rich packstone containing larger shell fragments in the lower part of the thin section (Vão Formation). Scale bar is 1 cm in all photographs.

mation from -0.75‰ to 0.18‰. The values are presented in Appendix 1 but also in Figures 4 and 10, respectively.

The values presented herein are comparable to the data published by Tammekänd et al. (2010) where the vast majority of the measured values of the carbon

isotope measurements falls between -1,5‰ and 0.0‰. In the Aseri Formation and the first ten centimetres of Vão Formation where this study overlaps with Tammekänd et al. (2010) the values are also quite similar. The values of the stable isotope measurements in this study could be affected post-depositionally by meteor-

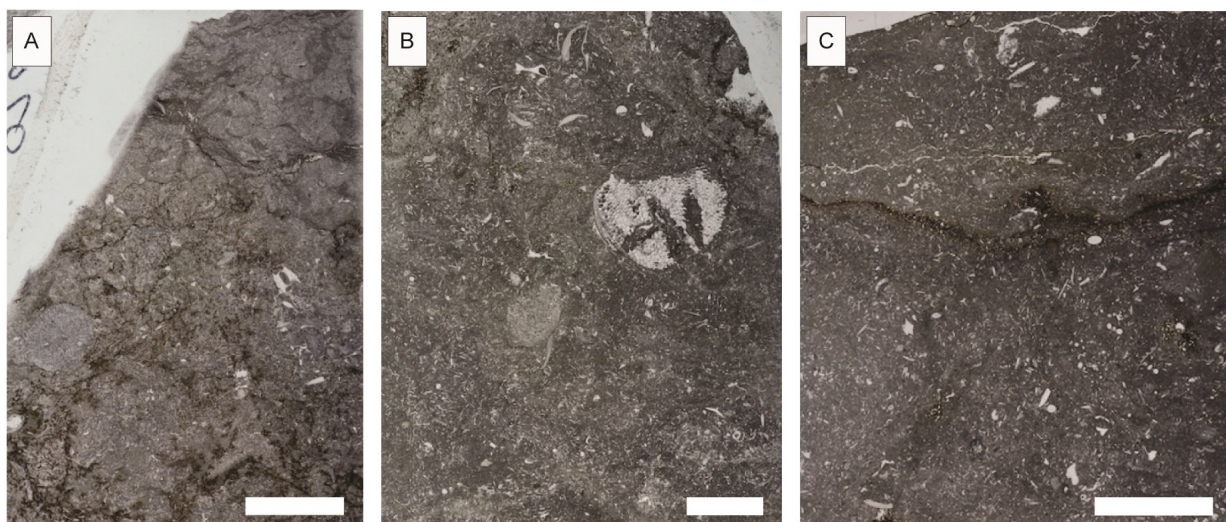


Fig. 13. Thin section micrographs of the Vão Formation from the Tabasalu road cut section. A. A brownish packstone. The brownish colour originates from muddy patches in the lower part of the thin section while in the middle and upper part there is a complex pattern of mud solution seams in a dolomitized area (Vão Formation). B. Patches of calcite cement throughout a brownish packstone thin section. Gastropod- and bryozoa fragments are also visible (Vão Formation). C. Trilobite- and echinoderm (gastropods also recognized) rich wackestone (Vão Formation). Scale bar is 1 cm in all photographs.

ic water and/or by dolomitization, which would lower the values (cf. Saltzman & Thomas 2012) and they will not be further discussed in this thesis.

## 9 Discussion

The sea level fluctuations in the Baltoscandian region are reflected in different ways throughout the rock formations of the Pakri peninsula and outside the city of Tabasalu. Detailed collection of rock samples has allowed for an interpretation of the general evolution of the depositional environment. Based on criteria such as carbonate microfacies, hardgrounds, and glauconite content, a discussion of relative sea level changes throughout each individual formation is presented in the following chapter. Relative sea level changes are based on the facies model presented by Harris et al. (2004) where a shallow shelf grain supported facies (containing grainstone and packstone) is interpreted as reflecting a depositional depth above the fair weather wave base. A middle shelf mixed facies (containing packstone and wackestone) is interpreted as reflecting a depositional depth between fair weather wave base and storm weather wave base.

### 9.1.1 Leetse Formation

The glauconite content in northern Estonia and the North Estonian Facies Belt is notable from the lower part of the Leetse Formation through the Pakri Formation. Most special in this respect is the Leetse Formation with its exclusively green glauconitic sands and muds. Glauconite is a hydrous potassium-iron-alumo-silicate mineral that forms only in marine environments. It is found in both carbonate and siliciclastic sediments. In modern oceans glauconite occurs between 50 and 500 m and is most common in outer-shelf to upper slope settings at depths between 200 and 300 m (Odin & Matter 1981). Chafetz & Reid (2000) were the first ones to point out that glauconite could form and accumulate in very shallow water depths of

no more than 10 meters and tidal flat tops. They did so by associating coarse-grained glauconitic mineral pellets of Cambro-Ordovician sediments in southwestern New Mexico and Central Texas with cross-stratified deposits and therefore shallow water environments. The cross stratification and its abundance points towards that individual pellets were deposited and covered by other laminae very rapidly (Chafetz & Reid 2000). Flügel (2010) states that the Cambro-Ordovician glauconite is most common in ramp and platform environments.

Glauconite formation is traditionally thought of as a slow depositional environment and has also often been connected to the formation of hardgrounds as is often the case in northern Estonia. The latter is also connected with low sedimentation rates or non-deposition for an extended period of time and erosion (Brett & Brookfield 1984).

Hardgrounds themselves can also be subject to mineralization such as oxidation depending on the environment it formed in. Glauconite mineralization occurs on shelf hardgrounds as does calcium phosphate and iron hydroxides like goethite. Glauconite in itself indicate a scarcity of fauna during the formation of the hardground (Lindström 1979). The mineralization itself is often around a millimetre in thickness and the boundary towards the unaffected limestone below is usually more diffuse while the upper one is generally sharper in character, sometimes truncating larger shell fragments etc.

In modern times there seems to be a clear link between slow or non-deposition and glauconite deposition. This implies that the newly formed glauconitic grains would stay at the water-sediment interface for an extended period of time. Chafetz & Reid (2000) cautioned against using modern environmental conditions such as depositional rate and depths as an analogue for the Cambro-Ordovician strata, suggesting that glauconitic minerals have a more complex history and origin than this.



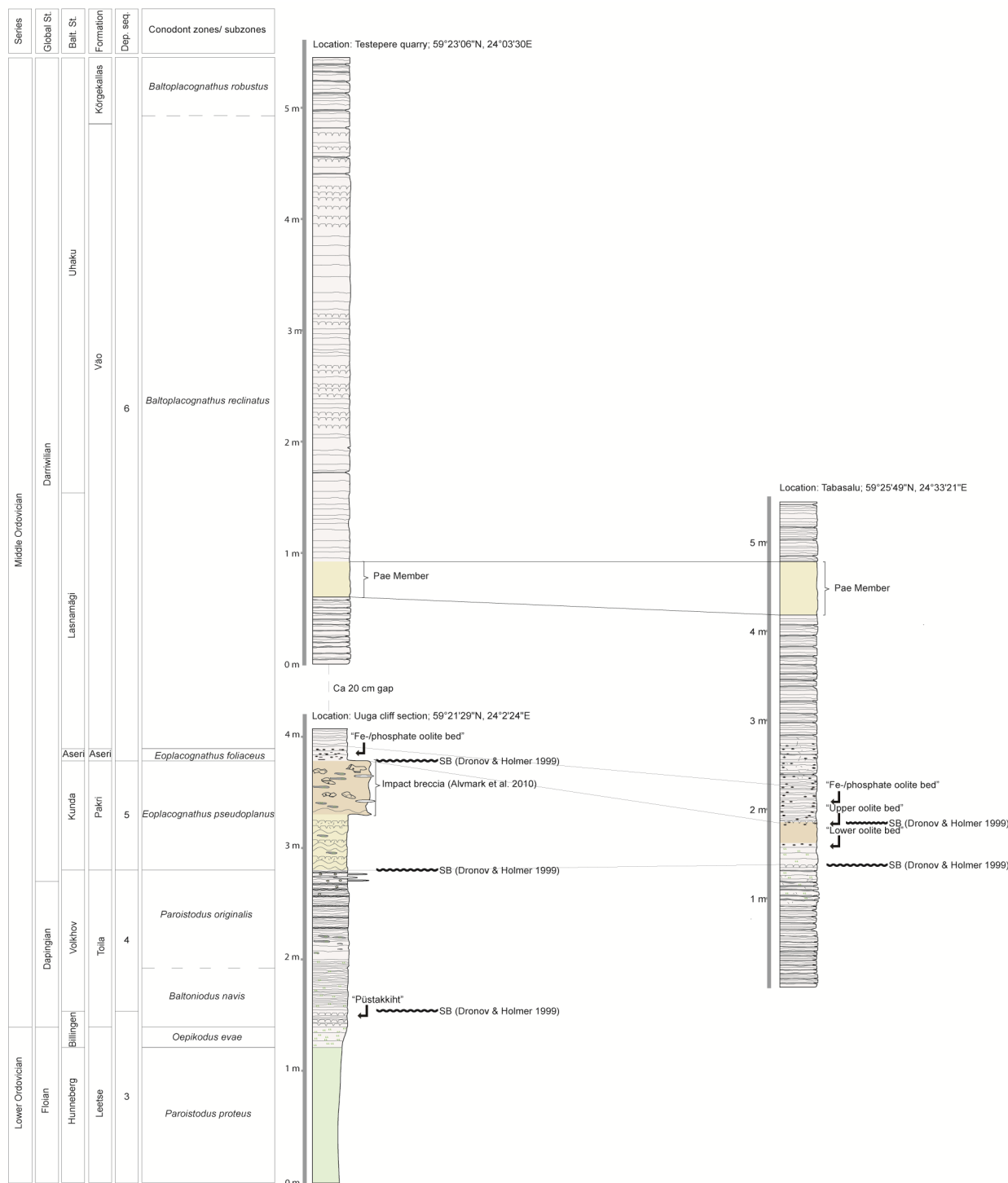


Fig. 14. Comparison of sedimentary logs from the Uuga cliff section and Testepere quarry to the Tabasalu road-cut. Conodont stratigraphy from Viira et al. (2001), Löfgren et al. (2005) and Hints et al. (2012). Depositional sequences are according to Dronov et al. (2011).

Amorosi (1993) recognized four groups while distinguishing between authigenic and detrital glauconite grains. Aside from being truly authigenic and not have undergone any transport glauconite grains can be perigenic and dispersed in the surrounding sediment. In the latter case the glauconite might have been transported in tides, storms and or currents. Detrital glauco-

nite can be transported either from submerged structural highs or derived from in situ reworking places. On the other hand it can also have been eroded from older stratigraphic levels. Grain size analysis has shown that sand and silt material of the Leetse Formation consists of detrital grains of siliciclastic minerals such as quartz feldspar and mica except for glauconite (Löfgren et al.

2005). Studies carried out along the north Estonian klint area show that there is a lower average content of potassium in the Leetse Formation around the Pakri peninsula compared to the north eastern part of Estonia, called the Saka section. This could also be indicative of a slightly faster sediment accumulation (Viira et al. 2006). Furthermore, Amorosi (1995) clarified that glauconite is not necessarily diagnostic of any specific systems tract in sequence stratigraphic terms. It is also in the uppermost part of the Leetse Formation that the *Oepikodus evae* conodont zone appears and it is visible as a positive shift in the  $\delta^{13}\text{C}$  record in the stratigraphical succession of Öland, Sweden. It is thought to indicate the onset of a global transgression (Calner et al. 2014).

### 9.1.2 Toila Formation

The gradual transition from the Leetse Formation to the Toila Formation and specifically the steady increase in calcite content and decrease in glauconite could indicate a deepening of the depositional environment but also slower deposition. It is interpreted as a highstand systems tract by Dronov & Holmer (1999) and the sequence boundary is set by the same authors by the “Püstakkiht” hardground complex, in the lower part of the Toila Formation.

Depositional sequence three (more specifically covering the Hunneberg and Billingen stages) covers 12 My but Dronov et al. (2011) opens up for the possibility of dividing it into several depositional sequences in the future due to difficulty of stratigraphic analysis. Although important and prominent stratigraphically, the sea level drop at “Püstakkiht” period is suggested by Dronov (2004) to be relatively small, only 10–20 meters. This further implies that the following Middle Ordovician could have been a highstand. Nielsen (2004) argues that the sea level fall was greater and thus the Middle Ordovician was a period of lowstand on a larger scale, corresponding to an approximately 80–100 meters lower sea level.

Thin sections from the lowermost part of the Toila Formation also show striking, partly abraded hardgrounds. The surfaces of hardgrounds can be broadly subdivided into two categories, abraded and corroded. Abraded surfaces are horizontally flat-topped whereas the corroded type is wavy or more irregular. The difference is inferably due to environmental differences; the flat-topped, abraded type formed where the sea floor was scoured by waves. It follows that this is formed above the fair weather wave base in a more high energy environment. This could be the case in the lower Toila Formation where there are also indications of a shallowing upwards of the basin at the very end as well as a period of several depositional breaks.

Another feature of the “Püstakkiht” hardground complex is that it is extensively bored. For further literature on these borings, see for example Ekdale & Bromley (2001). Borings like this occur in lithified sediments and thus cut across shells and grains. This gives some kind of indication to rate of sedimentation and speed of lithification. In an extremely slow depositional environment the sea floor has a chance to lithify and is likely to occasionally be scoured by currents or storms making it available for boring animals on the

sea floor. If the sedimentation rate is slightly higher and/ or cementation of the sea floor less complete, the sea floor might be burrowed (Shinn 1969).

The same thin section also reveals packstone indicative of mixed or possible grain supported facies. It would imply middle shelf environment or possibly shallow shelf environment where the abraded hardgrounds are visible.

Moving up the Toila Formation in the Uuga cliff section there is a hardground, PAK-S-3, with a partly clear-cut top surface, pointing towards some wave abrasion and a shallow environment in the bottom section. In the same interval there are grainstone lenses. Upsection there are marly lenses and nodular limestone that could possibly indicate a deepening of the basin. At the very top of the Uuga cliff section there are pyrite nodules and grainstone lenses which both point towards a shallowing of the environment and possibly also current activity since pyrite is believed to occur when currents erode in low oxygen environments (Baird & Brett 1986).

The Tabasalu road-cut with its common marly interbeds that increase upwards both in frequency and thickness suggests a deepening of the depositional environment throughout the Toila Formation. Hardgrounds in the upper part are corroded indicating long term low- or non-deposition below the fair weather wave base.

In accordance with Harris et al. (2004) this upper part of the Toila Formation would likely be middle shelf environment considering the mix of packstone and wackestone. Occasional presence of grainstone lenses in the Uuga cliff section, most notably at the very top of the Toila Formation is capped by an erosional surface that can be seen in Figure 3C. This would imply the lowest sea level and establishment of a shallow shelf environment.

### 9.1.3 Pakri Formation

The sea level drop between the Toila and Pakri formations is thought to have been large, up to 40 meters (Dronov 2004), which is partly why it is regionally accepted as a Series boundary. Directly above this sequence boundary is the reworked and dolomitized limestone of the Pakri Formation. The sugary, sandy texture possibly indicates a transgressive lag deposit. The formation of dolomite is a replacement of calcite by dolomite in calcareous sedimentary rocks through rock–fluid interactions where the fluid contains magnesium. A process like this can be either primary or secondary (occur syn- or postdeposition). The Estonian dolostone was formed shortly after deposition in shallow water or inner shelf environments (Teedumäe et al. 2006). The quick forming of dolomite can be seen through sedimentary and biogenic structures that have been preserved in the rock. Bitjukova et al. (1996) found that the Fe content has a positive correlation with the content of insoluble residue in the Ordovician rock. Thus they must be primary structures because the Fe and Mg must have been brought there before lithification by seawater. The primary dolomitization might point towards a very shallow environment and possibly also influenced by terrestrial fresh water. The reworking and the sugary sandy texture might indicate a

transgressive lag deposit following this period of shallow, freshwater environment.

The upper Pakri Formation in the Uuga cliff section constitutes a breccia with limestone clasts in a sandy matrix. The breccia, which likely derives from the underlying dolomitized limestone, consist of angular to subangular clasts up to 0.30 m in size. The clasts also show similar structures as is typical for the underlying unit, such as hardgrounds. This upper part of the Pakri Formation has been described by Alwmark et al. (2010) as the Osmussaar breccia and been interpreted as a direct consequence of a meteorite impact or as a result of an earthquake triggered by the impact.

The Tabasalu road-cut shows two horizons containing ooids. Ooids are generally thought to be indicative of shallow, high energy environments. Sturesson et al. (1999), however, points out that the origin of clay particles in the Pakri and Aseri formations in northern Estonia is volcanic ash. Further, they state that ooid formation for this reason need not necessarily mean an environment above the fair weather wave base. Where concentration of Fe in the ooids is high, samples are also rich in Mn. This, according to Teedumäe et al. (2006), is because of a higher primary supply of Fe and Mn as iron-manganese minerals are characteristic of the glauconitic carbonates of this unit. Thin sections of both study sites display corroded hardgrounds in the lower part of the Pakri Formation, indicative of slow net deposition, likely below the fair weather wave base. These angular or irregular surfaces are more common in slightly deeper marine settings. If they are very irregular with a high amplitude but also with a corroded top surface this might point towards a high energy environment and a shorter phase of creation (Flügel 2010). Smaller irregularities point towards formation in slightly deeper environments and a calmer environment where there is no wave action, like shelves and basins.

The thin sections also confirm the upwards increasing sand content and, specific to the Uuga cliff section, the reworking of the limestone and sandstone upsection. The mix of wackestone and packstone of the lower Pakri Formation in both sites studied would imply a mixed facies in accordance with Harris et al. (2004) and a middle shelf environment. Grainstone lenses in the upper Uuga cliff section might imply a more grain supported facies and a more shallow environment above the fair weather wave base.

#### 9.1.4 Aseri Formation

The Aseri Formation marks a lowstand systems tract according to Dronov & Holmer (1999). Both the Uuga cliff and the Tabasalu road-cut in this study show similar lithologies and the most striking features are the red ooids. Normally this indicates a high energy, shallow environment, but the Aserian ooids likely formed around the nuclei of volcanic ash particles (Sturesson et al. 1999) and it cannot be excluded that they formed in deeper, middle shelf, environment.

#### 9.1.5 The Vão and Kõrgekallas formations

The Vão Formation forms a transgressive systems tract (Dronov & Holmer 1999) together with the Kõrgekallas Formation. The Vão Formation is easily

separated into three members due to a distinct middle Pae Member of dolomitized brownish limestone. The lower part of the Vão Formation contains white ooids. Right underneath the Pae Member marly interbeds become common, possibly indicating a slight deepening of the basin. Most likely the Pae Member and the dolomite indicates a shallow water environment and possibly meteoric water input. The number of hardgrounds increases between two to three meters up, and around the 3.90 meter mark of the measured limestone section at the Testepere quarry (Fig. 5). The clear-cut character of the hardground in the PAK-S-18 thin section might indicate a very shallow environment above the fair weather wave base. Packstone dominates the main part of the Vão and Kõrgekallas formations with the exception at the uppermost meter where it changes towards a wackestone. In accordance with Harris et al. (2004) this environment would likely be grain supported facies and shallow shelf environment occasionally above the fair weather wave base. Evidence collected for this thesis points towards a shallow to middle shelf environment from Leetse Formation through the Kõrgekallas Formation. Microfacies analysis and studies of hardgrounds indicate a cyclic deposition of carbonates. The findings in this thesis seem to agree more with authors such as Dronov (2004) than Nielsen (2003). This can be especially noted between the Toila Formation and the Pakri Formation where the largest sea level fall likely occurred. This is indicated by the microfacies shifts as well as the erosional surface capping the Toila Formation.

## 9.2 Cool water carbonates and carbonate sedimentation in Baltoscandia

Through examining the lithologies in the Baltoscandian basin two broader phases of deposition are distinguished by Nielsen (2004) during the time period considered in this thesis. The first of these, ranging from the latest Tremadocian to mid-Floian, is characterized by slow deposition of cool-water carbonates that contain glauconite on the mid-shelf while on the inner shelf, extremely condensed glauconite-rich siliciclastic sediments are typical. The second phase ranged throughout the Middle Ordovician when mostly cool-water carbonates with successively less glauconite were deposited. Temperature and salinity are the two major controls of the composition of carbonate deposition according to Lees & Buller (1972) and Lees (1975). They realized that major differences between what was called cool-water carbonates and warm-water carbonates existed. Essentially it was seen at different latitudes that the differences are mainly based on the fact that cool-water carbonates are rich in bryozoas and barnacles while these animals are rare in warm water carbonates.

Normally, the further basinward the depositional environment is situated, the less carbonate production there is due to lack of organisms producing calcium carbonate. When a basin becomes too deep, the only sediments reaching distal areas are those of storms and redeposited material. In sedimentology this is evident through condensed sections overlying shallow water deposits. Condensed sections are caused by

very slow sedimentation rates and sometimes contain hardgrounds. Other environmental factors laying the foundation for hardgrounds are depletion of nutrients in the water, or dissolution of already semi-lithified sea floors.

The actual creation of the hardgrounds is mainly a result of aragonite and magnesian calcite precipitation directly from sea water (Wilson et al. 1992). Hardgrounds can be found in a variety of different environments, from deep marine settings to shallow subtidal environments and many more. Condensed sections are commonly indicators of maximum flooding surfaces at the base or top of a condensed section. This in turn is caused by a very rapid sea level rise where carbonate production is unable to keep up and is essentially drowned. Regardless of factors mentioned before, condensed sections indicate sediment starvation and flooding. On the other hand during relative sea level falls a shallow carbonate shelf will quickly become subaerially exposed. Depending on the climate, a karstified surface or sabkha is developed.

In the Baltoscandian region the Lower to Middle Ordovician carbonate sediments are mostly a mixture of skeletal sand and carbonate mud with terrigenous mud. Most of the bottom fauna is represented by brachiopods and echinoderms (such as crinoids or cystoids) that increased dramatically in diversity during this period. Trilobites existed since the Cambrian but still made up a healthy portion of the fauna. The limestone of Baltoscandia is primarily made up of the skeletal debris of these organisms. Beside these groups, conodonts were present and cephalopods were the main predator in these environments. Mud supported and grain supported carbonates exist but the mud supported is most common. The latter, where it exists, consists of winnowed skeletal sand with its mud component removed in diagenesis or never deposited. Skeletal remains of non-photosynthetic origin and, therefore, biotically controlled carbonate production dominates. This means that organisms will determine composition and form of the carbonate crystals produced as well as determining the start and termination of precipitation. There is generally little mud and where it exists, it is an abrasion product from larger carbonate shells. This is also why cool water carbonates generate ramps rather than rimmed shelves with reefs. It should also be noted that accumulation rates are very slow in cool-water factories compared to the warm-water counterpart.

Ooids do exist in smaller amounts but rather than being formed by “accretionary” aragonite it is formed by hydrous ferric oxide or chamosite (Jaanusson 1972). Because of this it can be suggested that the water temperature was relatively low and that these waters, therefore, could not precipitate aragonite. Consequently, Jaanusson (1972) states that the carbonate mud forming much of the Ordovician limestone in this region cannot have been precipitated from the seawater. Instead it must have been produced by particle size reduction and disintegration of skeletal material.

## 10 Conclusions

The Baltoscandian basin was a shallow marine environment with mostly smaller scale sea level fluctua-

tions and the investigated limestone consists mostly of a condensed limestone facies of the Middle Ordovician. Hardgrounds are extremely common throughout much of the section and occasionally show signs of abrasion. Together with a glauconite rich lime- and sandstone the hardgrounds indicate an extremely sediment starved depositional environment.

A carbonate microfacies curve has been constructed. This together with the primary sedimentary structures of the Leetse Formation indicates an overall deepening (mix of wackestone and packstone) of the marine environment in the Leetse Formation. Afterwards, in the Toila Formation, there was a shallow shelf environment turning in to a middle shelf environment at the end. Further upsection, throughout the Vão and Kõrgekallas formations carbonate microfacies analysis indicates an overall shallowing of the basin with a domination of packstone but also occasionally abraded hardgrounds.

Transgressions ending with a sea level drop can be seen throughout the formations studied. The top of Leetse Formation and the Toila Formation show an upwards decreasing content of glauconite due to a more continuous deposition of carbonates and a deepening of the marine environment. In the Toila Formation there is in addition an upwards increasing amount of marly interbeds indicative of a deepening environment. In the Vão Formation the transgression is apparent as the carbonate facies shifts from packstone to wackestone.

Glauconite is seen in Leetse through Pakri formations. At the Uuga cliff the sandy deposits of the Leetse Formation display cross stratification indicating deposition in a shallow, current-dominated environment. The content of glauconite decreases throughout the Pakri Formation.

Hardgrounds in the studied limestone of the Testepere quarry, the Uuga cliff section as well as the Tabasalu road-cut section occasionally are abraded, suggesting formation above the fair weather wave base. The latter ones occur in the beginning of Toila Formation (Uuga cliff) but also in the prominent hardground complex of the Vão Formation (Testepere quarry) and around the lower Oolite bed (Tabasalu road-cut).

## 11 Acknowledgements

I would like to thank my supervisor Mikael Calner for invaluable and helpful advice, positive encouragement and patience throughout the work with this thesis. I would also like to thank Oliver Lehnert for his help during field work in Estonia and valuable guidance when writing the thesis. Lastly, I would like to thank Jaak Nõlvak and colleagues at the Institute of Geology at Tallinn University of Technology for support and encouragement during my time spent in field and in Tallinn.

## 12 References

Alwmark, C., Schmitz, B. & Kirsimäe, K., 2010: The mid-Ordovician Osmussaar breccia in Estonia linked to the disruption of the L-chondrite parent body in the asteroid belt. *Geological Society of America Bulletin* 122, 1039-1046.

- Amorosi, M., 1993: Use of glauconites for stratigraphic correlation: a review and case studies. *Giornale di Geologia* 55, 117-137.
- Amorosi, M., 1995: Glaucony and sequence stratigraphy: a conceptual framework of distribution in siliciclastic sequences. *Journal of Sedimentary Research* B65, 419-425.
- Artyushkov, E. V., Lindström, M. & Popov, L. E., 2000: Relative sea-level changes in Baltoscandia in the Cambrian and early Ordovician: the predominance of tectonic factors and the absence of large scale eustatic fluctuations. *Tectonophysics* 320, 375-407.
- Artyushkov, E. V., Tesakov, Y. I. & Chekhovich, P. A., 2008: Ordovician sea-level change and rapid change in crustal subsidence rates in East Siberia and Baltoscandia. *Russian Geology and Geophysics* 49, 633-647.
- Baird, G. C. & Brett, C. E., 1986: Erosion of an anaerobic seafloor: Significance of reworked pyrite deposits from Devonian of New York State. *Palaeogeography, Palaeoclimatology, Palaeoecology* 57, 157-193.
- Bergström, S. M., Chen, X. U., Gutiérrez-Marco, J. C. & Dronov, A., 2009: The new chronostratigraphic classification of the Ordovician System and its relations to major regional series and stages and to  $\delta^{13}\text{C}$  chemostratigraphy. *Lethaia* 42, 97-107.
- Bityukova, A., Shogenova, A., Puura, V., Suuroja, K. & Saadre, T., 1996: Geochemistry of major elements in Middle Ordovician carbonate rocks: comparative analysis of alteration zones, North Estonia. *Proceedings of the Estonian Academy of Sciences, Geology* 45, 78-91.
- Brett, C. E. & Brookfield, M. E., 1984: Morphology, faunas and genesis of Ordovician hardgrounds from southern Ontario, Canada. *Palaeogeography, Palaeoclimatology, Palaeoecology* 46, 233-290.
- Calner, M., Lehnert, O., Wu, R., Dahlqvist, P. & Joachimski, M. M., 2014:  $\delta^{13}\text{C}$  chemostratigraphy in the Lower-Middle Ordovician succession of Öland (Sweden) and the global significance of the MDICE. *Gff* 136, 48-54.
- Chafetz, H. S. & Reid, A., 2000: Syndepositional shallow-water precipitation of glauconitic minerals. *Sedimentary Geology* 136, 29-42.
- Cocks, L. R. M. & Torsvik, T. H., 2002: Earth geography from 500 to 400 million years ago; a faunal and palaeomagnetic review. *Journal of the Geological Society of London* 159, part 6, 631-644.
- Cocks, L. R. M. & Torsvik, T. H., 2006: *European geography in a global context from the Vendian to the end of the Palaeozoic*. In: D. G. Gee & R. A. Stephenson (eds). *European Lithosphere Dynamics*. Geological Society, London, Memoirs, 32, 83-95.
- Dronov, A. V., 2004: Magnitude of sea-level changes in the Ordovician of Baltoscandia. In: O. Hints & L. Ainsaar (eds.) *WOGOGOB-2004: Conference materials*. Tartu University Press, Tartu. 21-22.
- Dronov, A. V., 2005: Introduction to the geology of the St. Petersburg region. In: A. V. Dronov, T. Tolmacheva, E. Raevskaya & M. Nestell (eds.) *Cambrian and Ordovician of St. Petersburg region -Guidebook of the pre-conference field trip. 6<sup>th</sup> Baltic stratigraphic conference*. St. Petersburg State University, St. Petersburg. 2-15.
- Dronov, A. V., Ainsaar, L., Kaljo, D., Meidla, T., Saadre, T. & Einasto, R., 2011: Ordovician of Baltoscandia: Facies, sequences and sea-level changes. In: J. C. Gutiérrez-Marco, I. Rábano & D. García-Bellido (eds.) *Ordovician of the World*. Vol. 14, 143-150. Publicaciones del Instituto Geológico y Minero de España, Serie, Cuadernos del Museo Geomin-Minero.
- Dronov, A. V. & Holmer, L. E., 1999: *Depositional sequences in the Ordovician of Baltoscandia*. *Geologica* 43, 133-136.
- Ekdale, A.A. & Bromley, R.G. 2001: Bioerosional innovation for living in carbonate hardgrounds in the Early Ordovician of Sweden. *Lethaia* 34, 1-12.
- Flügel, E., 2010: *Microfacies of Carbonate Rocks - Analysis, Interpretation and Application, 2<sup>nd</sup> edition*. Springer-Verlag Berlin Heidelberg, 984 pp.
- Haq, B. U. & Schutter, S. R., 2008: A chronology of Paleozoic sea-level changes. *Science* 322, 64-68.
- Harris, M.T., Sheehan, P.M., Ainsaar, L., Hints, L., Männik, P., Nõlvak, J. & Bubel, M., 2004: Upper Ordovician sequences of western Estonia. *Palaeogeography, Palaeoclimatology, Palaeoecology* 210, 135-142.
- Hints, O., Viira, V. & Nõlvak, J., 2012: Darrivilian (Middle Ordovician) conodont biostratigraphy in NW Estonia. *Estonian Journal of Earth Sciences* 61, 210-226.
- Jaanusson, V., 1972: Constituent analysis of an Ordovician limestone from Sweden. *Lethaia* Vol 5, 217-237.
- Jaanusson, V., 1976: Faunal dynamics in the Middle Ordovician (Viruan) of Balto-Scandia. In: M. G. Bassett (ed.) *The Ordovician System: proceedings of a Palaeontological Association symposium, Birmingham, September 1974*. University of Wales Press and National Museum of Wales, Cardiff. 301-326.
- Jaanusson, V. & Bergström, S. M., 1980: Middle Ordovician faunal spatial differentiation in Baltoscandia and the Appalachians. *Alcheringa: An Australasian Journal of Palaeontology* 4, 89-110.
- Kaljo, D., Martma, T. & Saadre, T., 2007: Post-Hunnebergian Ordovician carbon isotope trend in Baltoscandia, its environmental implications and some similarities with that of Nevada. *Palaeogeography, Palaeoclimatology, Palaeoecology* 245, 138-155.
- Kiipli, E., Kiipli, T. & Kallaste, T., 2009: Reconstruction of currents in the Mid-Ordovician-Early Silurian central Baltic Basin using geochemical and mineralogical indicators. *Geology* 37, 271-274.

- Lees, A., 1975: Possible influence of salinity and temperature on modern shelf carbonate sedimentation. *Marine Geology* 19, 159-198.
- Lees, A. & Buller, A. T., 1972: Modern temperate-water and warm-water shelf carbonate sediments contrasted. *Marine Geology* 13, 67-73.
- Lindström, M., 1963: Sedimentary folds and the development of limestone in an early Ordovician sea. *Sedimentology* 2, 243-292.
- Lindström, M., 1979: Diagenesis of lower ordovician hardgrounds in Sweden. *Geologica et Paleontologica* 13, 9-30.
- Löfgren, A., Viira, V. & Mens, K., 2005: Conodont biostratigraphy and sedimentary history in the upper Tremadoc at Uuga, Cape Pakri, NW Estonia. *Gff* 127, 283-293.
- Miller, K. G., Kominz, M. A., Browning, J. V., Wright, J. D., Mountain, G. S., Katz, M. E., Sugarman, P. J., Cramer, B. S., Christie-Blick, N. & Pekar, S. F., 2005: The Phanerozoic Record of Global Sea-Level Change. *Science* 310, 1293-1298.
- Meidla, T. Ainsaar, L., & Tinn, O., 1998. Volkhov stage in north Estonia and sea level changes. *Proceedings of the Estonian Academy of Sciences Geology* 1998 47, 141-147.
- Meidla, T. & Ainsaar, L., 2004. On the Ordovician System in Estonia. In: O. Hints & L. Ainsaar (eds.) *WOGOGO-2004: Conference materials*. Tartu University Press, Tartu. 107-111.
- Meidla, T., Ainsaar, L. & Hints, O., 2014: The Ordovician System in Estonia. In: H. Bauert, O. Hints, T. Meidla & P. Männik (eds.) *4<sup>th</sup> Annual Meeting of IGCP 591*. University of Tartu, Tartu. 116-122.
- Munnecke, A., Calner, M., Harper, D. a. T. & Servais, T., 2010: Ordovician and Silurian sea-water chemistry, sea level, and climate: A synopsis. *Palaeogeography, Palaeoclimatology, Palaeoecology* 296, 389-413.
- Nestor, H., Soesoo, A., Linna, A., Hints, O. & Nõlvak, J., 2007: The Ordovician in Estonia & southern Finland. MTÜ Geoguide Baltoscandia, Tallinn. 1-32.
- Nichols, G., 2009: *Sedimentology and Stratigraphy, 2<sup>nd</sup> Edition*. Wiley-Blackwell. 419 pp.
- Nielsen, A.T., 1995: Trilobite biostratigraphy, palaeoecology and systematics of the Komstad Limestone and the Huk Formation (Lower Ordovician), southern Scandinavia. *Fossils and Strata* 38, 374.
- Nielsen, A. T., 2003: Ordovician sea-level changes: potential for global event stratigraphy In: G. L. Albanesi, M. S. Beresi & S. H. Peralta (eds.) *Ordovician from the Andes: Proceedings of the 9<sup>th</sup> International Symposium on the Ordovician System*. INSUGEO: Serie Correlación Geológica 17. 445-450.
- Nielsen, A. T., 2004: Ordovician sea-level changes in Baltoscandia. In: O. Hints & L. Ainsaar (eds.) *WOGOGO-2004: Conference materials*. Tartu University Press, Tartu. 69-70.
- Nõlvak, J., Hints, O. & Männik, P., 2006: Ordovician timescale in Estonia: recent developments. *Proceedings of the Estonian Academy of Sciences Geology* 2006 55, 95-108.
- Odin, G. S. & Matter, A., 1981: De glauconiarum origine. *Sedimentology* 28, 611-641.
- Plint, A. G., Eyles, N., Eyles, C. H. & Walker, R. G., 1992: Control of sea level change. In R. G. Walker & N. P. James. (eds): *Facies models: response to sea level change*, 15-25. Geological Association of Canada, St Johns.
- Põldsaar, K. & Ainsaar, L., 2014: Extensive soft-sediment deformation structures in the early Darriwilian (Middle Ordovician) shallow marine siliciclastic sediments formed on the Baltoscandian carbonate ramp, northwestern Estonia. *Marine Geology* 356, 111-127.
- Raukas, A. & Teedumäe, A., 1997: *Geology and Mineral Resources of Estonia*. Estonian Academy Publishers, Tallinn, 433 pp.
- Saltzman, M. R. & Thomas, E. 2012: Carbon isotope stratigraphy. In F. Gradstein, J. Ogg, M. D. Schmitz & G. Ogg (eds.): *The Geologic Time Scale 2012*, Elsevier, B. V., 207-232.
- Shinn, E. A., 1969: Submarine Lithification of Holocene Carbonate Sediments in the Persian Gulf. *Sedimentology* 12, 109-144..
- Sturesson, U., 1995: Llanvirnian (Ord.) iron ooids in Baltoscandia: element mobility, REE distribution patterns, and origin of the REE. *Chemical Geology* 125, 45-60.
- Sturesson, U., Dronov, A. & Saadre, T., 1999: Lower Ordovician iron ooids and associated oolitic clays in Russia and Estonia: a clue to the origin of iron oolites? *Sedimentary Geology* 123, 63-80.
- Tammekänd, M. Hints, O. & Nõlvak, J., 2010: Chitinozoan dynamics and biostratigraphy in the Vão Formation (Darriwilian) of the Uuga Cliff, Pakri Peninsula, NW Estonia. *Estonian Journal of Earth Sciences* 59, 25.
- Teedumäe, A., Shogenova, A. & Kallaste, T., 2006: Dolomitization and sedimentary cyclicity of the Ordovician, Silurian, and Devonian rocks in South Estonia. *Proceedings of the Estonian Academy of Sciences* 55, 67-87.
- Viira, V., Löfgren, A., Mägi, S. & Wickström, J., 2001: An Early to Middle Ordovician succession of conodont faunas at Mäekalda, northern Estonia. *Geological Magazine* 138, 699-718.
- Viira, V., Mens, K. & Nemliher, J., 2006: Lower Ordovician leetse formation in the north estonian klint area. *Proceedings of the Estonian Academy of Sciences* 55, 156-174.
- Wilson, M. A., Palmer, T. J., Guensburg, T. E., Finton, C. D. & Kaufman, L. E., 1992: The development of an Early Ordovician hardground community in response to rapid sea floor calcite precipitation.pdf. *Lethaia* 25, 19-34.

## 13 Appendix

$\delta^{13}\text{C}$  data from the Uuga cliff section.

Height (m)	Sample no.	Formation	$\delta^{13}\text{C}$
0,01	PAK01	Toila Fm.	-0,61
0,03	PAK02	Toila Fm.	-0,05
0,045	PAK03	Toila Fm.	-0,27
0,06	PAK04	Toila Fm.	-0,15
0,08	PAK05	Toila Fm.	-0,33
0,11	PAK06	Toila Fm.	-0,30
0,13	PAK07	Toila Fm.	-0,34
0,16	PAK08	Toila Fm.	0,19
0,19	PAK09	Toila Fm.	-0,43
0,26	PAK10	Toila Fm.	-1,19
0,33	PAK11	Toila Fm.	-2,24
0,36	PAK12	Toila Fm.	0,10
0,43	PAK13	Toila Fm.	0,18
0,46	PAK14	Toila Fm.	-1,36
0,54	PAK15	Toila Fm.	-0,61
0,58	PAK16	Toila Fm.	-0,33
0,64	PAK17	Toila Fm.	-1,04
0,67	PAK18	Toila Fm.	-0,54
0,74	PAK19	Toila Fm.	-1,33
0,79	PAK20	Toila Fm.	0,04
0,83	PAK21	Toila Fm.	-0,55
0,855	PAK22	Toila Fm.	0,05
0,89	PAK23	Toila Fm.	-0,62
1,03	PAK24	Toila Fm.	0,21
1,10	PAK25	Toila Fm.	-0,73
1,19	PAK26	Toila Fm.	0,08
1,27	PAK27	Toila Fm.	-0,16
1,30	PAK28	Toila Fm.	-0,18
1,32	PAK29	Toila Fm.	0,16
1,36	PAK30	Toila Fm.	-1,14
1,40	PAK31	Toila Fm.	0,17
1,45	PAK32	Pakri Fm.	-1,84
1,51	PAK33	Pakri Fm.	-1,91
1,56	PAK34	Pakri Fm.	-1,45
1,62	PAK35	Pakri Fm.	-2,31
1,71	PAK36	Pakri Fm.	-2,43
1,79	PAK37	Pakri Fm.	-2,29
1,89	PAK38	Pakri Fm.	-2,14
2,40	PAK39	Aseri Fm.	-1,23
2,405	PAK40	Aseri Fm.	-1,40
2,43	PAK41	Aseri Fm.	-1,28

$\delta^{13}\text{C}$  data from the Uuga cliff section (*continued*)

Height (m)	Sample no.	Formation	$\delta^{13}\text{C}$
2,455	PAK42	Aseri Fm.	-0,93
2,475	PAK43	Aseri Fm.	-1,07
2,49	PAK44	Aseri Fm.	-0,98
2,505	PAK45	Lasnamägi Fm.	-0,76
2,53	PAK46	Lasnamägi Fm.	-0,89
2,59	PAK47	Lasnamägi Fm.	-0,13
2,66	PAK48	Lasnamägi Fm.	-0,57

$\delta^{13}\text{C}$  data from the Tabasalu road cut section.

Height (m)	Sample no.	Formation	$\delta^{13}\text{C}$
0,085	KAL01	Toila Fm.	-0,43
0,18	KAL02	Toila Fm.	-0,30
0,29	KAL03	Toila Fm.	0,11
0,40	KAL04	Toila Fm.	0,40
0,49	KAL05	Toila Fm.	-0,76
0,62	KAL06	Toila Fm.	-0,26
0,72	KAL07	Toila Fm.	-0,68
0,98	KAL08	Toila Fm.	-0,63
1,07	KAL09	Toila Fm.	-0,19
1,20	KAL10	Toila Fm.	-0,01
1,26	KAL11	Toila Fm.	-0,06
1,33	KAL12	Toila Fm.	0,48
1,37	KAL13	Toila Fm.	-0,75
1,45	KAL14	Pakri Fm.	-0,82
1,54	KAL15	Pakri Fm.	-0,61
1,57	KAL16	Pakri Fm.	-0,64
1,60	KAL17	Pakri Fm.	-0,39
1,72	KAL18	Pakri Fm.	-0,10
1,76	KAL19	Pakri Fm.	0,51
1,78	KAL20	Pakri Fm.	0,44
1,84	KAL21	Pakri Fm.	0,25
1,88	KAL22	Aseri Fm.	-0,004
1,95	KAL23	Aseri Fm.	0,05
2,02	KAL24	Aseri Fm.	0,05
2,09	KAL25	Aseri Fm.	-0,08
2,17	KAL26	Aseri Fm.	0,08
2,22	KAL27	Aseri Fm.	-0,02
2,28	KAL28	Aseri Fm.	-0,03
2,32	KAL29	Lasnamägi Fm.	0,04
2,45	KAL30	Lasnamägi Fm.	-0,35



$\delta^{13}\text{C}$  data from the Tabasalu road cut (continued)

Height (m)	Sample no.	Formation	$\delta^{13}\text{C}$
2,45	KAL30	Lasnamägi Fm.	-0,35
2,49	KAL31	Lasnamägi Fm.	-0,75
2,53	KAL32	Lasnamägi Fm.	-0,63
2,60	KAL33	Lasnamägi Fm.	0,10
2,65	KAL34	Lasnamägi Fm.	-0,58
2,76	KAL35	Lasnamägi Fm.	-0,40
2,86	KAL36	Lasnamägi Fm.	-0,03
2,91	KAL37	Lasnamägi Fm.	-0,16
2,98	KAL38	Lasnamägi Fm.	-0,23
3,05	KAL39	Lasnamägi Fm.	-0,06
3,14	KAL40	Lasnamägi Fm.	-0,19
3,21	KAL41	Lasnamägi Fm.	0,07
3,27	KAL42	Lasnamägi Fm.	0,0006
3,28	KAL43	Lasnamägi Fm.	-0,19
3,34	KAL44	Lasnamägi Fm.	-0,14
3,42	KAL45	Lasnamägi Fm.	-0,04
3,48	KAL46	Lasnamägi Fm.	0,05
3,58	KAL47	Lasnamägi Fm.	0,06
3,66	KAL48	Lasnamägi Fm.	0,02
3,74	KAL49	Lasnamägi Fm.	-0,06
3,89	KAL50	Lasnamägi Fm.	0,11
3,97	KAL51	Lasnamägi Fm.	0,10
4,015	KAL52	Lasnamägi Fm.	-0,09
4,09	KAL53	Lasnamägi Fm.	0,19
4,17	KAL54	Lasnamägi Fm.	-0,13
4,27	KAL55	Lasnamägi Fm.	0,14
4,345	KAL56	Lasnamägi Fm.	-0,20
4,43	KAL57	Lasnamägi Fm.	-0,08
4,53	KAL58	Lasnamägi Fm.	-0,22
4,61	KAL59	Lasnamägi Fm.	-0,004
4,68	KAL60	Lasnamägi Fm.	0,005
4,79	KAL61	Lasnamägi Fm.	0,18
4,92	KAL62	Lasnamägi Fm.	0,03
5,02	KAL63	Lasnamägi Fm.	-0,02
5,06	KAL64	Lasnamägi Fm.	-0,27
5,14	KAL65	Lasnamägi Fm.	0,10
5,235	KAL66	Lasnamägi Fm.	-0,002
5,29	KAL67	Lasnamägi Fm.	-0,04
5,435	KAL68	Lasnamägi Fm.	0,10



## Tidigare skrifter i serien

### ”Examensarbeten i Geologi vid Lunds universitet”:

437. Nordlander, Lina, 2015: Borrningsteknikens påverkan vid provtagning inför dimensionering av formationsfilter. (15 hp)
438. Fennvik, Erik, 2015: Resistivitet och IP-mätningar vid Äspö Hard Rock Laboratory. (15 hp)
439. Pettersson, Johan, 2015: Paleoeologisk undersökning av Triberga mosse, sydöstra Öland. (15 hp)
440. Larsson, Alfred, 2015: Mantelplymer - realitet eller *ad hoc*? (15 hp)
441. Holm, Julia, 2015: Markskador inom skogsbruket - jordartens betydelse (15 hp)
442. Åkesson, Sofia, 2015: The application of resistivity and IP-measurements as investigation tools at contaminated sites - A case study from Kv Renen 13, Varberg, SW Sweden. (45 hp)
443. Lönsjö, Emma, 2015: Utbredningen av PFOS i Sverige och världen med fokus på grundvattnet – en litteraturstudie. (15 hp)
444. Asani, Besnik, 2015: A geophysical study of a drumlin in the Åsnen area, Småland, south Sweden. (15 hp)
445. Ohlin, Jeanette, 2015: Riskanalys över pesticidförekomst i enskilda brunnar i Sjöbo kommun. (15 hp)
446. Stevic, Marijana, 2015: Identification and environmental interpretation of microtextures on quartz grains from aeolian sediments - Brattforsheden and Vittskövle, Sweden. (15 hp)
447. Johansson, Ida, 2015: Is there an influence of solar activity on the North Atlantic Oscillation? A literature study of the forcing factors behind the North Atlantic Oscillation. (15 hp)
448. Halling, Jenny, 2015: Inventering av sprickmineraliseringar i en del av Sorgenfrei-Tornquistzonen, Dalby stenbrott, Skåne. (15 hp)
449. Nordas, Johan, 2015: A palynological study across the Ordovician Kinnekulle. (15 hp)
450. Åhlén, Alexandra, 2015: Carbonatites at the Alnö complex, Sweden and along the East African Rift: a literature review. (15 hp)
451. Andersson, Klara, 2015: Undersökning av slugtestsmetodik. (15 hp)
452. Ivarsson, Filip, 2015: Hur bildades Bushveldkomplexet? (15 hp)
453. Glommé, Alexandra, 2015:  $^{87}\text{Sr}/^{86}\text{Sr}$  in plagioclase, evidence for a crustal origin of the Hakefjorden Complex, SW Sweden. (45 hp)
454. Kullberg, Sara, 2015: Using Fe-Ti oxides and trace element analysis to determine crystallization sequence of an anorthositenorite intrusion, Ålgön SW Sweden. (45 hp)
455. Gustafsson, Jon, 2015: När började plattetektoniken? Bevis för plattetektoniska processer i geologisk tid. (15 hp)
456. Bergqvist, Martina, 2015: Kan Ölands grundvatten öka vid en uppdämning av de utgrävda diken genom strandvallarna på Ölands östkust? (15 hp)
457. Larsson, Emilie, 2015: U-Pb baddeleyite dating of intrusions in the southeasternmost Kaapvaal Craton (South Africa): revealing multiple events of dyke emplacement. (45 hp)
458. Zaman, Patrik, 2015: LiDAR mapping of presumed rock-cored drumlins in the Lake Åsnen area, Småland, South Sweden. (15 hp)
459. Aguilera Pradenas, Ariam, 2015: The formation mechanisms of Polycrystalline diamonds: diamondites and carbonados. (15 hp)
460. Viehweger, Bernhard, 2015: Sources and effects of short-term environmental changes in Gullmar Fjord, Sweden, inferred from the composition of sedimentary organic matter. (45 hp)
461. Bokhari Friberg, Yasmin, 2015: The paleoceanography of Kattegat during the last deglaciation from benthic foraminiferal stable isotopes. (45 hp)
462. Lundberg, Frans, 2016: Cambrian stratigraphy and depositional dynamics based on the Tomten-1 drill core, Falbygden, Västergötland, Sweden. (45 hp)
463. Flindt, Anne-Cécile, 2016: A pre-LGM sandur deposit at Fiskarheden, NW Dalarna - sedimentology and glaciotectionic deformation. (45 hp)
464. Karlatou-Charalampopoulou, Artemis, 2016: Vegetation responses to Late Glacial climate shifts as reflected in a high resolution pollen record from Blekinge, south-eastern Sweden, compared with responses of other climate proxies. (45 hp)
465. Hajny, Casandra, 2016: Sedimentological study of the Jurassic and Cretaceous sequence in the Revinge-1 core, Scania. (45 hp)

- hp)
466. Linders, Wictor, 2016: U-Pb geochronology and geochemistry of host rocks to the Bastnäs-type REE mineralization in the Riddarhyttan area, west central Bergslagen, Sweden. (45 hp)
467. Olsson, Andreas, 2016: Metamorphic record of monazite in aluminous migmatitic gneisses at Stensjöstrand, Sveconorwegian orogen. (45 hp)
468. Liesirova, Tina, 2016: Oxygen and its impact on nitrification rates in aquatic sediments. (15 hp)
469. Perneby Molin, Susanna, 2016: Embryologi och tidig ontogeni hos mesozoiska fisködlor (Ichthyopterygia). (15 hp)
470. Benavides Höglund, Nikolas, 2016: Digitization and interpretation of vintage 2D seismic reflection data from Hanö Bay, Sweden. (15 hp)
471. Malmgren, Johan, 2016: De mellankambriska oelandicuslagren på Öland - stratigrafi och facietyper. (15 hp)
472. Fouskopoulos Larsson, Anna, 2016: XRF-studie av sedimentära borrhärdar - en metodstudie av programvarorna Q-spec och Tray-sum. (15 hp)
473. Jansson, Robin, 2016: Är ERT och Tidsdomän IP potentiella karteringsverktyg inom miljögeologi? (15 hp)
474. Heger, Katja, 2016: Makrofossilanalys av sediment från det tidig-holocena undervattenslandskapet vid Haväng, östra Skåne. (15 hp)
475. Swierz, Pia, 2016: Utvärdering av vattenkemisk data från Borgholm kommun och dess relation till geologiska förhållanden och markanvändning. (15 hp)
476. Mårdh, Joakim, 2016: WalkTEM-undersökning vid Revingehed provpumpningsanläggning. (15 hp)
477. Rydberg, Elaine, 2016: Gummigranulat - En litteraturstudie över miljö- och hälsopåverkan vid användandet av gummigranulat. (15 hp)
478. Björnfors, Mark, 2016: Kusterosion och äldre kustdyners morfologi i Skälderviken. (15 hp)
479. Ringholm, Martin, 2016: Klimatutlöst matbrist i tidiga medeltida Europa, en jämförande studie mellan historiska dokument och paleoklimatarkiv. (15 hp)
480. Teilmann, Kim, 2016: Paleomagnetic dating of a mysterious lake record from the Kerguelen archipelago by matching to paleomagnetic field models. (15 hp)
481. Schönström, Jonas, 2016: Resistivitets- och markradarmätning i Ängelholmsområdet - undersökning av korrosiva markstrukturer kring vattenledningar. (15 hp)
482. Martell, Josefin, 2016: A study of shock-metamorphic features in zircon from the Siljan impact structure, Sweden. (15 hp)
483. Rosvall, Markus, 2016: Spår av himlakroppskollisioner - bergarter i nedlagsskrattar med fokus på Mien, Småland. (15 hp)
484. Olausson, My, 2016: Resistivitets- och IP-mätningar på den nedlagda deponin Gustavsfält i Halmstad. (30 hp)
485. Plan, Anders, 2016: Markradar- och resistivitetsmätningar - undersökningar utav korrosionsförhöjande markegenskaper kring fjärrvärmeledningar i Ängelholm. (15 hp)
486. Jennerheim, Jessica, 2016: Evaluation of methods to characterise the geochemistry of limestone and its fracturing in connection to heating. (45 hp)
487. Olsson, Pontus, 2016: Ekologiskt vatten från Lilla Klåveröd: en riskinventering för skydd av grundvatten. (15 hp)
488. Henriksson, Oskar, 2016: The Dynamics of Beryllium 10 transport and deposition in lake sediments. (15 hp)
489. Brådenmark, Niklas, 2016: Lower to Middle Ordovician carbonate sedimentology and stratigraphy of the Pakri peninsula, north-western Estonia. (45 hp)



# LUNDS UNIVERSITET

Geologiska institutionen  
Lunds universitet  
Sölvegatan 12, 223 62 Lund